Quantitative Economics 7 (2016), 821–857 1759-7331/20160821

Robust dynamic energy use and climate change

Xin Li
International Monetary Fund

Borghan Narajabad
Board of Governors, Federal Reserve System

Ted Temzelides
Department of Economics and James A. Baker III Institute for Public Policy, Rice University

We study a dynamic stochastic general equilibrium model in which agents are concerned about *model uncertainty* regarding climate change. An externality from greenhouse gas emissions damages the economy's capital stock. We assume that the mapping from climate change to damages is subject to uncertainty, as opposed to risk, and we use robust control to study efficiency and optimal policy. We obtain a sharp analytical solution for the implied environmental externality and characterize dynamic optimal taxation. The optimal tax that restores the socially optimal allocation is Pigouvian. We study optimal output growth in the presence and in the absence of concerns about model uncertainty, and find that these can lead to substantially different conclusions regarding the optimal emissions and the optimal mix of fossil fuel. In particular, the optimal use of coal will be significantly lower on a robust path, while the optimal use of oil/gas will edge down.

Keywords. Robustness, climate change, model uncertainty, dynamic taxation.
JEL classification. D81, H21, Q54.

1. Introduction

We study optimal taxation in a dynamic stochastic economy in which there is uncertainty about the effects of climate change. So as to introduce concerns about uncertainty, we employ the setup in Hansen and Sargent (2008). We then investigate how optimal taxation depends on the concentration of carbon in the atmosphere in the presence

Xin Li: XLi4@imf.org
Borghan Narajabad: borghan.narajabad@frb.gov
Ted Temzelides: tedt@rice.edu

We thank two anonymous referees, as well as Lars Peter Hansen, Nicolas Querou, Rick van der Ploeg, participants at the 2013 Midwest Macro Conference, the Econometric Society Summer 2013 Meeting, the ASSA 2014 Meeting, the SED 2014 Meeting, the CESifo 2014 Energy and Climate Economics Conference, the 14th LAGV Conference in Aix-en-Provence, Carnegie–Mellon University, and the USA/IAEE 33rd North American Conference for their comments and suggestions. Opinions expressed do not necessarily reflect those of the Federal Reserve System. The views expressed in this paper are those of the author(s) and do not necessarily represent the views of the IMF, its Executive Board, or IMF management.

DOI: 10.3982/QE463

of such concerns. Moreover, we show that model uncertainty has significant quantitative implications regarding the optimal greenhouse gas (GHG) emissions and, in particular, the optimal mix of fossil fuel used.

The use of fossil fuel and the resulting rise of GHG concentrations are widely accepted to cause climate change, resulting in adverse effects on the current and future capital stock and output of the world economy. The precise relationship between fossil fuel use and economic damage is complex due to several factors, including uncertainty about productivity growth in different sources of energy, the future elasticity of substitution between renewable and fossil fuel sources, the exact amount of fossil fuel available, and the effect from the dynamics of carbon concentrations. Moreover, there is substantial uncertainty about the resulting damages to capital stock and output. After all, manmade climate change is unprecedented, and there is an ongoing heated debate about its potential effects. These range from the effect of the rise of sea levels on coastal cities to the risks of large-scale human migration resulting in conflict. Given that the introduction of even one source of model uncertainty complicates the model significantly, in this paper we will focus on this last source. We will study the implications of model uncertainty for economic damages, the optimal fuel mix, and economic growth. While model uncertainty (also referred to as Knightian uncertainty or ambiguity) has been studied in economics mainly in the context of macroeconomics and financial economics, we believe that the unprecedented effects from manmade climate change make this approach quite relevant in the context of environmental economics.

So as to model the climate effects from the externality associated with GHG emissions, we employ the framework used in Golosov, Hassler, Krusell, and Tsyvinski (2014; GHKT hereafter). While they assume that the mapping from climate change to damages is subject to risk, in our model this mapping is subject to uncertainty. While restrictive, this framework provides a tractable setup that allows us to derive an analytical solution for a benchmark case. We then develop a recursive method for solving the model computationally under more general assumptions.

An important difference between our results and GHKT is in relation to their main finding. The core theoretical result in GHKT is that, when expressed as a proportion of gross domestic product (GDP), the optimal tax on emissions depends only on the discount factor, the measure of the expected damages, and the depreciation of the carbon concentration. In particular, the tax rate in their model is independent of the stochastic value of the future output and of the stock of carbon in the atmosphere. The following assumptions are necessary for their result: (i) utility is logarithmic, which implies a constant saving rate; (ii) the climate damages are proportional to GDP and have constant elasticity with respect to the level of the carbon concentration; and (iii) the stock of carbon is linear in past and current emissions.[1] We will demonstrate that, even under these restrictive assumptions, once we consider model uncertainty, the expected level of damages is *no longer sufficient* to determine the optimal tax. Specifically, we will show that

[1] For a related paper, see van den Bijgaart, Gerlagh, and Liski (2013). Rezai and van der Ploeg (2014) consider more general specifications that include temperature lags, population growth, and damages that are not proportional to GDP. We will restrict attention to the GHKT structure in what follows.

the robust optimal tax rises as the level of GHG concentration increases, even though the expected damages remain unchanged.

As is standard in the robust control literature, our paper postulates that the decision-maker views his model as an approximation, termed the *approximating model*. We then formulate the problem of optimal fossil fuel use as a two-person zero-sum dynamic game. In each stage, a social planner (a representative household in the decentralized version) maximizes social welfare (lifetime utility) by choosing the level of energy, consumption, labor, and capital investment. Subsequently, a malevolent player chooses alternative distributions so as to minimize the respective payoff. Intuitively, the malevolent player leads the decision-maker to search for decision rules that are robust to a worst-case scenario about model misspecification. As is standard, we assume that the malevolent player pays a penalty, which is a decreasing function of the social planner's (the representative household's) concern about model uncertainty.

We find that the robust optimal tax that restores the optimal allocation in the presence of model uncertainty is Pigouvian. However, unlike GHKT, the robust optimal tax *does* depend on the GHG concentration. In the presence of concern about model uncertainty, a higher GHG concentration increases the cost of model misspecification. The robust optimal emission tax rises to account for this additional effect.

In the calibrated version of the model, we find that an increase in the concern about model uncertainty causes a significant decline in the use of *coal*, while the use of *oil/gas* is only slightly delayed. This difference is partly due to the abundance of coal and the higher emissions resulting from generating energy from coal. Even when we assume a more constrained stock of coal, model uncertainty implies that the optimal use of coal is reduced. In contrast, the scarcity effect dominates the model uncertainty effect when determining the optimal use of oil/gas. However, when we consider a higher level of the initial stock of oil/gas, the concern about model uncertainty substantially discourages the use of this oil/gas as well.[2] Finally, the concern about model uncertainty does not have a sizable effect on the robust optimal path of *green* energy use, since this type of energy does not create emissions. However, as green energy, coal, and oil/gas are substitutes, uncertainty indirectly affects the use of green energy, through its effect on coal and oil/gas. Nevertheless, this indirect effect does not generate noticeable implications for the robust optimal path of green energy use.

The main implication of the concern about model uncertainty would be realized if the damages from climate change evolve according to the worst-case model. Under one of our two specifications for the approximating model, the carbon concentration surpasses a breakout threshold after 20 years on the nonrobust path. That is, if the nonrobust path is followed and the worst-case scenario is realized, the damages could become beyond repair after 20 years. However, under our alternative specification, damages are always bounded on the nonrobust path. Nevertheless, if the worst-case scenario is realized, then the difference between the robust and nonrobust path could reach 50 percent

[2]Additional future sources of oil/gas include unconventional sources from shale and deep water, as well as methane hydrates. See Boswell and Collett (2011), Hartley, Medlock, Temzelides, and Zhang (2016), and references therein for a more detailed discussion on total estimated fossil fuel resources.

of the output within 200 years. Needless to say, avoiding the damage under the worst-case scenario is the main reason for the difference between the robust and nonrobust paths when there is concern about model uncertainty.

There is a growing body of literature studying the interplay between the environment and the macroeconomy. Acemoglu, Aghion, Bursztyn, and Hemous (2012) study a model that connects growth and environmental issues. Nordhaus and Boyer (2000) and Stern (2007) point to the importance of uncertainty.[3] Bommier (2006) and Bommier and Rochet (2006) uncover a link between risk aversion and discounting in life-cycle models. Bommier, Lanz, and Zuber (2015) introduce the possibility of economic collapse whose hazard rate depends on the stock of pollution using a model without additively separable preferences. They show that multiplicatively separable preferences lead to a higher social value of catastrophic risk reduction. Gerlagh and Liski (2014) investigate how environmental policy responds to the delayed arrival of information about damages. In a recent paper, Anderson, Brock, Hansen, and Sanstad (2014) explicitly deal with model uncertainty in the context of climate models.[4] Earlier related modeling that precedes robust control includes Jacobson (1973), Whittle (1981, 2002), and van der Ploeg (1993). As discussed in Hansen and Sargent (2010), in the presence of misspecification, it makes sense to introduce learning, which makes an interesting extension of the present paper for future research.[5]

The paper proceeds as follows. Section 2 describes the general model. Section 3 imposes a set of simplifying assumptions that allows us to solve the model analytically. Section 4 solves a more detailed version of the model and allows us to study the implications of the concern about uncertainty for the use of different types of fossil fuel. Section 5 concludes. The Appendix contains some related technical material.

2. The economic environment

In this section, we will describe the economic environment leading to the "robust planner's problem." This setup will allow us to study optimal policy in the presence of concerns about model uncertainty in dealing with climate change resulting from GHG. Later, we will show how the solution to the robust planner's problem can be implemented as a decentralized market equilibrium.

Time, t, is discrete and the horizon is infinite. The economy is populated by a unit measure continuum of infinite-lived representative agents with utility

$$E_0 \sum_{t=0}^{\infty} \beta^t u(C_t),$$

[3] GHKT discuss in detail the connection of their model to Nordhaus's dynamic integrated climate economy (DICE) model. Two differences in the climate modeling are in the time profile of the depreciation of carbon emissions and in the assumption that the full temperature response to atmospheric carbon is immediate.

[4] See also Funke and Paetz (2010).

[5] Our work contributes to the literature of applications of robust control in economics in two ways. First, we explore a class of models under a nonquadratic objective and nonlinear constraints. Second, we employ the exponential, in addition to the normal distribution as the approximating distribution.

where u is a standard concave period utility function, C_t represents final goods consumption in period t, and $\beta \in (0,1)$ is the discount factor. The final goods sector uses energy, E, capital, K, and labor, N, to produce output. Labor supply is inelastic. The economy's capital stock is assumed to depreciate fully.[6] Henceforth, the end-of-period capital before interacting with the climate factor through the process described below, denoted by $\tilde{K}$, is given by

$$\tilde{K}_{t+1} = Y_t - C_t.$$

There are four production sectors. The final goods sector, indexed by $i = 0$, produces the consumption good. The corresponding production function is given by $Y = F(K, N_0, E)$. Thus, in addition to capital and labor, production of the final good requires the use of energy, E. The three energy-producing sectors for oil/gas, coal, and green energy (labeled by $i = 1, 2, 3$, respectively) produce energy amounts E_1, E_2, and E_3 (measured in carbon equivalents). We assume

$$E = \left(\kappa_1 E_1^\rho + \kappa_2 E_2^\rho + \kappa_3 E_3^\rho\right)^{1/\rho},$$

where $\rho < 1$ denotes the elasticity of substitution between the different types of energy. The parameter κ_i captures the relative efficiency of the different types of energy and is normalized by setting $\sum_{i=1}^3 \kappa_i = 1$.[7] The oil/gas sector is assumed to produce oil/gas at zero cost. We denote by R the total oil/gas energy stock, and we impose the resource constraint $R_t \geq 0$ for all t. Note that the oil/gas stock evolves according to $R' = R - E_1$. Both the coal and the green energy sectors use linear technologies

$$E_i = A_i N_i, \quad i = 2, 3.$$

We will denote the labor productivity growth by A_N; that is, $N' = A_N N$. We follow GHKT in modeling a simplified carbon cycle as follows. The variable S (measured in units of carbon content) represents the GHG concentration in the atmosphere in excess of the preindustrial level. We denote by P and T the permanent and temporary components of S, respectively, which evolve according to the equations

$$\begin{aligned} P' &= P + \phi_L(E_1 + E_2), \\ T' &= (1-\phi)T + (1-\phi_L)\phi_0(E_1 + E_2), \\ S' &= P' + T', \end{aligned}$$

where ϕ_L denotes the fraction of GHG emission that adds to the permanent atmospheric GHG concentration, $1 - \phi_0$ is the fraction that is absorbed immediately from the temporary component, and ϕ is the fraction of the temporary component of the GHG concentration that is absorbed every period.

[6] We will concentrate on a long-term horizon and abstract from short-term dynamics, such as fluctuations of capital accumulation over the short run. Each period will be calibrated to be 10 *years*, which partially justifies the 100 percent capital depreciation assumption.

[7] Since coal produces more carbon per unit of energy than oil/gas, we will impose that $\kappa_1 > \kappa_2$.

We introduce model uncertainty regarding the effect of climate change through a stochastic variable, γ, which reduces the end-of-period capital stock $\tilde{K}'$ by a factor of $h(S', \gamma)$ to K'.[8] That is,

$$K' = h\big(S', \gamma\big)\tilde{K}'.$$

We use $\pi(\gamma)$ to denote the approximating distribution of γ, while $\hat{\pi}(\gamma)$ denotes the welfare-minimizing distribution and $m(\gamma) = \frac{\hat{\pi}(\gamma)}{\pi(\gamma)}$ is the likelihood ratio. The distance, ϱ, between $\hat{\pi}(\gamma)$ and $\pi(\gamma)$ is measured by *relative entropy*:[9]

$$\begin{aligned}\delta &\equiv \varrho\big(\hat{\pi}(\gamma), \pi(\gamma)\big) \equiv \boldsymbol{E}\big[m(\gamma)\log m(\gamma)\big] \equiv \hat{\boldsymbol{E}}\big[\log m(\gamma)\big] \\ &\equiv \int \big[m(\gamma)\log m(\gamma)\big]\pi(\gamma)\,\mathrm{d}\gamma.\end{aligned} \tag{1}$$

As is standard in the robust control literature, the concern about model uncertainty is represented by a two-person zero-sum dynamic game in which, after observing the choice of a social planner, a "malevolent player" chooses the worst specification of the model in each period. Our attention will be restricted to a particular type of equilibrium, the so-called Markov perfect (or *feedback*) equilibrium. This equilibrium is *strongly time consistent*. At the beginning of a period, the state (K, N, P, T, R) is revealed. Then the planner chooses $(C, E_i, N_i, \tilde{K}', P', T', S', R')$ so as to maximize expected social welfare. After observing the planner's choice, the malevolent player chooses an alternative distribution $\hat{\pi}(\gamma)$ or, equivalently, $m(\gamma)$ to minimize expected welfare. The malevolent nature's deviation from the approximating distribution is *penalized* by adding $\alpha\varrho(\hat{\pi}(\gamma), \pi(\gamma))$ to the planner's objective function, where α represents the magnitude of the deviation "punishment." Recall that ϱ is the distance between the approximating distribution, π, and the malevolent player's choice of distribution, $\hat{\pi}$. Therefore, a larger α punishes the malevolent player's deviation from the planner's approximating distribution by adding a larger amount to the planner's problem. Thus, a higher α makes a large deviation less likely, which is equivalent to a lower concern about robustness.

[8] This specification implicitly captures model uncertainty about the *composition* of two mappings: from carbon concentrations to temperature changes, and then from temperature changes to damages. While γ directly affects output in GHKT, we assume that γ adversely affects the economy's capital stock. The two assumptions are identical under a Cobb–Douglas production function and an exponential damage function (which we assume throughout this paper). Our specification allows us to assume that the social planner moves before nature in each period. The resulting max-min game is easier to analyze. To see the equivalence with GHKT, assume that the economy enters a period with capital k and carbon concentration S. In GHKT, the final goods production is given by $A_0 e^{-\gamma S} K^\theta N_0^{1-\theta-\nu} E^\nu$, while in our model it is given by $A_0(e^{-\gamma S}K)^\theta N_0^{1-\theta-\nu} E^\nu = A_0 e^{-\theta\gamma S} K^\theta N_0^{1-\theta-\nu} E^\nu$. These expressions are identical if γ is scaled up by a factor of $\frac{1}{\theta}$.

[9] Relative entropy, also called the *Kullback–Leibler distance*, is widely used in robust control as a measure of the distance between two probability distributions. It is not a metric, as it violates symmetry and triangle inequality. However, it is a pre-metric, satisfying $\varrho(\hat{\pi}(\gamma), \pi(\gamma)) \geq 0$ and $\varrho(\pi(\gamma), \pi(\gamma)) = 0$. Relative entropy has a positive semidefinite Hessian matrix, which allows us to derive the worst-case distribution, $\hat{\pi}(\gamma)$, for the max-min problem, given the approximating distribution, $\pi(\gamma)$.

Incorporating the malevolent player's decision, the social planner's problem can be written as

$$
\begin{aligned}
&V(K,N,P,T,R;A)\\
&\quad=\max_{\{C,E_i,N_i,\tilde{K}',P',T',S',R'\}}\min_{m(\gamma)}\Bigg\{u(C)\\
&\qquad+\beta\int\big[m(\gamma)V\big(K',N',P',T',R'\big)+\alpha m(\gamma)\log m(\gamma)\big]\pi(\gamma)\,\mathrm{d}\gamma\Bigg\},
\end{aligned}
\tag{2}
$$

s.t.

$$
\begin{aligned}
&E_i=A_iN_i,\quad i=2,3,\\
&E=\big(\kappa_1E_1^{\rho}+\kappa_2E_2^{\rho}+\kappa_3E_3^{\rho}\big)^{1/\rho},\\
&N=N_0+N_2+N_3,\\
&\tilde{K}'=F(K,N_0,E)-C,\\
&K'=h\big(S',\gamma\big)\tilde{K}',\\
&R'=R-E_1\geq 0,\\
&N'=A_NN,\\
&P'=P+\phi_L(E_1+E_2),\\
&T'=(1-\phi)T+(1-\phi_L)\phi_0(E_1+E_2),\\
&S'=P'+T',\\
&1=\int m(\gamma)\pi(\gamma)\,\mathrm{d}\gamma.
\end{aligned}
$$

The social planner's problem can be solved analytically under a set of additional assumptions. We will first focus on the analytical solution. While restrictive, the solution provides intuition that will carry over when we relax these assumptions and solve the calibrated model computationally. We will also discuss decentralization and show that the socially optimal allocation can be restored by imposing appropriate fossil fuel taxes on the energy-producing sector.

3. The baseline analytical solution

In this section, we will impose a set of assumptions that will allow us to fully solve the model analytically. As we shall see, certain aspects of the solution remain instructive in the next section, when the restrictive assumptions are dropped and the model is solved numerically. The assumptions are as follows:

A1. The period utility function is given by $u(C)=\log(C)$.

A2. The production function is given by $F(K,N_0,E)=K^{\theta}N_0^{1-\theta-\nu}E^{\nu}$.

A3. The damage function is given by $h(S',\gamma)=e^{-S'\gamma}$.

A4. The approximating distribution for γ is exponential, with mean λ^{-1} and variance λ^{-2}; that is, $\pi(\gamma) = \lambda e^{-\lambda\gamma}$.[10]

A5. There is no population growth or, equivalently, labor productivity improvement. The aggregate labor supply is normalized to 1. That is, $A_N = 1$ and $N = 1$ in all periods.

A6.1. We have $\phi_L = 0$.[11]

A6.2. We have $\phi = 0$.

A7. There is a single fossil energy sector producing oil/gas at zero cost. Production is subject to a resource feasibility constraint: $R' \geq 0$. As a result, $N_1 = 0$ and $N_0 = N$.

A8. The resource feasibility constraint is not binding.

We will first solve the social planner's problem. We will then discuss the decentralized problem and show that the socially optimal allocation can be restored by implementing fossil fuel taxes on the energy-producing sector.

Under A1–A8, the social planner's problem can be rewritten as

$$\begin{aligned} &V(K,S) \\ &\quad = \max_{C,E,\tilde{K}',S'} \min_{m(\gamma)} \left\{ u(C) + \beta \int \left[m(\gamma) V\left(K',S'\right) + \alpha m(\gamma) \log m(\gamma) \right] \pi(\gamma)\, \mathrm{d}\gamma \right\}, \\ &\text{s.t.} \\ &\quad \tilde{K}' = K^{\theta} E^{\nu} - C, \\ &\quad K' = e^{-S'\gamma} \tilde{K}', \\ &\quad S' = S + \phi_0 E, \\ &\quad 1 = \int m(\gamma)\pi(\gamma)\, \mathrm{d}\gamma. \end{aligned} \tag{3}$$

(4)

To solve this problem, we first guess and then verify that $V(\cdot)$ takes the form

$$V\left(K',S'\right) = f\left(S'\right) + \bar{A}\log\left(K'\right) + \bar{D} = f\left(S'\right) + \bar{A}\log\left(e^{-S'\gamma}\cdot\tilde{K}'\right) + \bar{D}, \tag{5}$$

where $\bar{A}$ and $\bar{D}$ are undetermined coefficients. The functional form for $f(\cdot)$ will be derived when we solve the minimizing malevolent player's problem.

[10]The exponential distribution with mean λ^{-1} is the maximum-entropy distribution among all continuous distributions supported in $[0,\infty]$ that have mean λ^{-1}. The worst-case distribution for γ is also exponential, with mean $(\lambda^*)^{-1}$ and variance $(\lambda^*)^{-2}$, where $\lambda^* = \lambda(1-\Delta S'^*) = \lambda(1-\Delta\phi_0 c_E)(1-\Delta S)$. That is, $\pi^*(\gamma) = \lambda^* e^{-\lambda^*\gamma}$. Since $\lambda^* = \lambda(1-\Delta S'^*) < \lambda$, the worst-case mean of γ, $(\lambda^*)^{-1}$, is strictly greater than the approximating mean, λ^{-1}.

[11]If $\phi_L > 0$, we need to depict the dynamics of P and T separately before we sum them to obtain the dynamics of S. Assuming that $\phi_L = 0$ allows us to express the dynamics of S without the need to consider P and T separately. That is, $S' = (1-\phi)S + \phi_0 E$. Moreover, A6.1 and A6.2 imply that $S' = S + \phi_0 E$, which is necessary for an analytical solution.

We define the robustness problem (the *inner minimization problem*) by

$$\mathcal{R}(V)\big(\tilde{K}', S'\big) = \min_{m(\gamma)} \int \big[m(\gamma)V\big(K', S'\big) + \alpha m(\gamma)\log m(\gamma)\big]\pi(\gamma)\,\mathrm{d}\gamma, \tag{6}$$

s.t.

$$K' = e^{-S'\gamma}\tilde{K}',$$

$$1 = \int m(\gamma)\pi(\gamma)\,\mathrm{d}\gamma.$$

This is the problem of the malevolent player, who chooses a deviation from the approximating distribution, $m(\gamma)$. This choice is made after the robust planner has chosen the installed level of capital, $\tilde{K}'$, and the atmospheric concentration of GHG, S'. As a result, the realization of the damage parameter, γ, comes from the distribution $\hat{\pi}(\gamma) = m(\gamma)\cdot\pi(\gamma)$, instead of the planner's initial approximating distribution $\pi(\gamma)$.

The first-order condition for $m(\gamma)$ from (6) combined with (5) implies

$$\hat{\pi}^*(\gamma) = m^*(\gamma)\pi(\gamma) = \lambda^* e^{-\lambda^*\gamma}, \tag{7}$$

where $\lambda^* = \lambda(1-\Delta S')$ and $\Delta = \frac{\bar{A}}{\alpha\lambda}$. In other words, the *worst-case* distribution for γ is an exponential distribution with distorted mean $(\lambda^*)^{-1}$ and variance $(\lambda^*)^{-2}$. If the GHG concentration exceeds a threshold value, $S' \geq \frac{1}{\Delta}$, then the system cannot be "robustified," in the sense that the value of the game goes to negative infinity.[12] We call $\frac{1}{\Delta}$ the *breakout threshold*.

Substituting the solution (7) into the minimization problem (6) and using the guessed value function (5), we obtain

$$\mathcal{R}(V)\big(\tilde{K}', S'\big) = f\big(S'\big) + \bar{A}\log\big(\tilde{K}'\big) + \bar{D} + H\big(S'; \alpha, \bar{A}\big),$$

where $H(S'; \alpha, \bar{A})$ denotes the robust version of the externality from GHG emissions and is given by

$$H\big(S'; \alpha, \bar{A}\big) = \alpha\log\big(1-\Delta S'\big) = \alpha\log\bigg(1 - \frac{\bar{A}}{\alpha\lambda}S'\bigg). \tag{8}$$

Next, we solve the optimal choice problem of the robust planner (the *outer maximization problem*), which is given by

$$V(K, S) = \max_{\{C, E, \tilde{K}', S'\}} \big\{\log(C) + \beta\mathcal{R}(V)\big(\tilde{K}', S'\big)\big\}$$

or, equivalently,

$$f(S) + \bar{A}\log(K) + \bar{D}$$
$$= \max_{C,E}\big\{\log(C) + \beta\big[f\big(S'\big) + \bar{A}\log\big(\tilde{K}'\big) + \bar{D} + \alpha\log\big(1-\Delta S'\big)\big]\big\},$$

[12] However, if the economy starts with an initial $S_0 < \frac{1}{\Delta}$, then S_t will converge to $\frac{1}{\Delta}$ as $t \to +\infty$.

s.t.

$$\tilde{K}' = K^{\theta}E^{\nu} - C,$$
$$S' = S + \phi_0 E.$$

The first-order conditions imply

$$C = \frac{K^{\theta}E^{\nu}}{1+\beta\bar{A}}, \tag{9}$$
$$-\phi_0\left[\frac{\partial f(S')}{\partial S'} + \frac{-\alpha\Delta}{1-\Delta S'}\right] = \frac{1+\beta\bar{A}}{\beta}\cdot\frac{\nu}{E}. \tag{10}$$

We guess that $f(S) = \bar{B}\log(1-\Delta S)$, where $\bar{B}$ is an undetermined coefficient. As a result, (10) can be simplified as

$$E = \frac{\nu(\beta\bar{A}+1)}{\beta\phi_0\Delta(\alpha+\bar{B})}\cdot\left(1-\Delta S'\right).$$

After some derivations, we obtain

$$\bar{A} = \frac{\theta}{1-\beta\theta},$$
$$\bar{B} = \frac{1}{1-\beta}\left[\alpha\beta + \frac{\nu}{1-\beta\theta}\right].$$

The expression for $\bar{D}$ is more complicated and less intuitive. Substituting $\bar{A} = \frac{\theta}{1-\beta\theta}$ into the first-order conditions, we obtain the optimal allocation. We summarize the above discussion in the following proposition.

PROPOSITION 3.1. *Assume that* A1–A8 *hold. The two-person zero-sum dynamic game described by* (3) *has a feedback* (*Markov perfect*) *equilibrium. The equilibrium strategies are given by*

$$C^* = (1-\beta\theta)K^{\theta}E^{*\nu} = (1-\beta\theta)K^{\theta}\left[c_E(1-\Delta S)\right]^{\nu}, \tag{11}$$
$$E^* = c_E(1-\Delta S), \tag{12}$$
$$S'^* = S + \phi_0 c_E(1-\Delta S),$$
$$\hat{\pi}^*(\gamma) = \lambda^* e^{-\lambda^*\gamma},$$

where $c_E = \frac{\nu(1-\beta)}{[\beta\alpha(1-\beta\theta)+\nu]\phi_0\Delta}$ *and* $\lambda^* = \lambda(1-\Delta S'^*)$ *for* $\Delta = \frac{\theta}{(1-\beta\theta)\alpha\lambda}$.

Certain properties of the optimal allocation are worth noting. The value function $V(K,S)$ is increasing in K, decreasing in S, and jointly concave in K and S. The value of $\bar{A}$ is the same as in the model without concern about model uncertainty, that is, $\frac{\partial\bar{A}}{\partial\alpha} = 0$. Both oil/gas use, E^*, and next-period GHG concentration, S'^*, are affine functions of the current GHG concentration, S. Moreover, E^* is decreasing in S, and S'^* converges to

$\frac{1}{\Delta} = \frac{\alpha\lambda(1-\beta\theta)}{\theta}$. It can be shown that, given S, both E^* and S'^* are increasing functions of α. This relationship is intuitive since a greater α implies a larger resulting penalty from a deviation of γ from its approximating distribution; thus, there is a lower concern about model uncertainty. Note that C^* is affected by S only through E^*, due to the logarithmic utility assumption. As a result, a greater concern about model uncertainty will lower both E^* and C^*.

The marginal value of the externality from one unit of emissions in terms of utility evaluated on the optimal path, (K'^*, S'^*), is given by

$$\lambda^s = -\beta \frac{\partial V(K', S')}{\partial E}\bigg|_{K'^*, S'^*} = \frac{\nu}{(1-\beta\theta)E^*} = \frac{\nu}{(1-\beta\theta)c_E(1-\Delta S)}. \tag{13}$$

The optimal oil/gas use, E^*, is a decreasing function of the GHG concentration, S, and a decreasing function of the concern about model uncertainty, captured inversely by α. Therefore, the externality from emissions, λ^s, is increasing in both the GHG concentration and the concern about model uncertainty. The intuition behind this result is straightforward. As the GHG concentration increases, a deviation from the approximating distribution becomes more attractive for the malevolent player. Thus, the robust planner would find emitting more costly because of the malevolent player's reaction to a higher GHG concentration. A higher concern about model uncertainty, captured by a lower α, would make the externality from carbon emissions more pronounced. As we will show in our numerical investigation, this result holds under more general assumptions.

Robust control modeling can be introduced in a variety of ways. In this model, we have used a closed-loop zero-sum dynamic game in which the social planner moves first in each period. Alternatively, we could construct a game with the same information structure by interchanging the order of max and min in equation (3). The two games differ only in terms of the timing protocol. However, both lead to the same (unique) feedback saddle-point equilibrium if certain conditions are satisfied. More precisely, if A1–A8 hold, the objective in (3) is strictly concave in C and E, and strictly convex in $m(\gamma)$. Consequently, the two closed-loop zero-sum dynamic games admit the same unique pure-strategy saddle-point Nash equilibrium, which is the one described in Proposition 3.1.

3.1 *Robust energy consumption*

The binding limit on oil/gas use in our model comes not from the resource constraint A8, but rather from the externality generated by carbon emissions.[13] As a result, the concern about model uncertainty is the major determinant of oil/gas use. Using $S_{t+1} = S_t + \phi_0 E_t$, we arrive at the expression for aggregate oil/gas extraction,

$$\sum_{t=0}^{\infty} E_t = \lim_{t\to\infty} \phi_0^{-1}(S_t - S_0) = \phi_0^{-1}\left(\frac{1}{\Delta} - S_0\right),$$

[13]Our benchmark model is similar to the oil/gas regime in GHKT, except that we assume that the resource constraint is not binding.

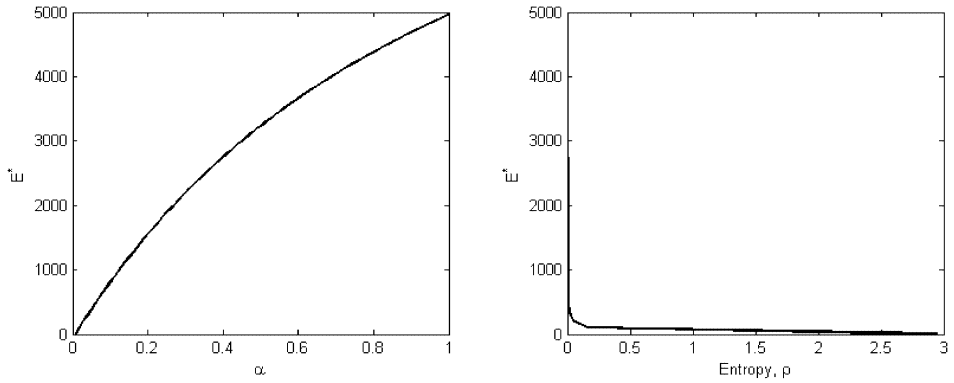

FIGURE 1. Robustness concerns and optimal use of fossil fuel.

where $\lim_{t\to\infty} S_t = \frac{1}{\Delta}$ follows from $S'^* = S + \phi_0 c_E(1 - \Delta S)$. Thus, the resource constraint is not binding if and only if the aggregate oil/gas reserves are greater than $\phi_0^{-1}(\frac{1}{\Delta} - S_0)$, which would be another way of expressing A8.

The left panel of Figure 1 shows how the robust optimal oil/gas use, E^*, varies across different values of the penalty parameter, α, whose inverse captures the concern about model uncertainty. Recall that a higher penalty makes the malevolent player less likely to alter the distribution governing the damage parameter, γ. A higher α corresponds to a lower concern about model uncertainty, which, in turn, makes the robust planner more comfortable with a higher level of oil/gas use, resulting in higher carbon emissions.

The distance (relative entropy) between $\hat{\pi}^*(\gamma)$ and $\pi(\gamma)$ is given by

$$\delta \equiv \varrho\big(\hat{\pi}^*(\gamma), \pi(\gamma)\big) = \log\big(1 - \Delta S'^*\big) + \frac{\Delta S'^*}{1 - \Delta S'^*},$$

where $\varrho(\hat{\pi}^*(\gamma), \pi(\gamma))$ can be viewed as the maximum deviation allowed from the approximating model, $\pi(\gamma)$, given the penalty parameter, α. Since $\Delta = \frac{\theta}{\alpha\lambda(1-\beta\theta)}$, it follows that the relative entropy, δ, is decreasing in the penalty parameter, α. The right panel of Figure 1 shows how E^* changes as we relax δ, allowing for additional uncertainty about the approximating model. In the Appendix, we show that $\frac{\partial E^*}{\partial \delta}|_{\delta=0} = -\infty$. That is, even an infinitesimal concern about model uncertainty can cause a significant drop in the optimal energy extraction.

3.2 *Decentralization*

Next, we demonstrate how the robust optimal allocation can be implemented by imposing a tax on emissions. Recall that the extraction cost of energy (the cost of creating emissions) is assumed to be zero. Thus, if the tax per unit of emissions is set at τ_t and the resulting proceeds, $\tau_t E_t$, are rebated in a lump sum, agents will equate the tax cost to the direct benefit they receive per unit of emissions. More formally, we have

$$\tau_t = p_t = \frac{\partial F(K_t, E_t)}{\partial E_t} = \nu K_t^{\theta} E_t^{\nu-1}.$$

The above expression captures the one-to-one relationship between emissions, or equivalently energy, E_t, and the tax rate, τ_t. To achieve the optimal emissions level, as given by $E_t^* = c_E(1 - \Delta S)$ in equation (12), we must impose $\tau_t^* = \nu c_E^{\nu-1}(1 - \Delta S_t)^{\nu-1} K_t^{\theta}$. It is straightforward to show that $\tau_t^* = \frac{\lambda^s}{u'(C_t^*)}$, where C_t^* is the optimal consumption, given by (11), and λ^s is the externality from one unit of emissions in terms of utility, given by (13). That is, the robust optimal tax on emissions is equal to the corresponding GHG externality, as measured in units of the consumption good.

The optimal consumption, C_t^*, is achieved under the optimal tax, as we show using the representative agent's problem. Since we have established a one-to-one relationship between E_t and τ_t, we may assume without loss of generality that the planner chooses $E_t = E_t^*$. In addition, since $E_t^* = c_E(1 - \Delta S)$, we can similarly assume that the emissions/energy choice is given as a function of the atmospheric GHG concentration, that is, $E = E(S)$. Given the choice of E, aggregate capital stock K, (accumulated) GHG concentration S, and a malevolent player with penalty parameter α, an agent with starting capital k solves the problem

$$V(k, K, S) = \max_{c, \tilde{k}'} \min_{\hat{\pi}(\gamma)} \left\{ \log(c) + \beta \hat{E}_\gamma \left[V\left(k', K', S'\right) + \alpha \log\left(\frac{\hat{\pi}(\gamma)}{\pi(\gamma)} \right) \right] \right\},$$

s.t.

$$c + \tilde{k}' = r(K, S)k + \tau(K, S)E(S) + \pi^{\text{profit}},$$

$$\tilde{K}' = G(K, S),$$

$$k' = e^{-\gamma S'} \tilde{k}',$$

$$K' = e^{-\gamma S'} \tilde{K}',$$

$$S' = S + \phi_0 E(S).$$

Capital income in the above expression is given by $r(K, S) = \theta K^{\theta-1}[E(S)]^{\nu}$. Per-unit tax on energy/emissions is given by $\tau(K, S) = \nu K^{\theta}[E(S)]^{\nu-1}$. Hence, the lump-sum tax rebate is $\tau(K, S)E(S)$. The representative firm's profit is $\pi^{\text{profit}} = \theta K^{\theta}[E(S)]^{\nu} - r(K, S) \cdot K$, while the equilibrium transition law for the aggregate capital stock is given by $\tilde{K}' = G(K, S)$. Here, (k, K, S) stands for the beginning-of-period state and $(\tilde{k}', \tilde{K}', S')$ stands for the end-of-period state. The next period's GHG concentration, S', evolves by adding the unabsorbed fraction of new emissions, $\phi_0 E(S)$, which is a function of the current level of GHG concentration. Notice that $(\tilde{k}', \tilde{K}')$ is not equal to the beginning-of-next-period state, (k', K'), due to the capital deterioration resulting from the climate effect, as captured by the factor $e^{-\gamma S'}$. Moreover, $\hat{E}_\gamma$ is calculated with respect to the worst-case distribution for γ, $\hat{\pi}(\gamma)$, as chosen by the malevolent player. Since the minimizing player moves after the maximizing player, the worst distribution is, in general, conditional on the end-of-period state, $(\tilde{k}', \tilde{K}', S')$.

It can be shown that the optimal consumption sequence satisfies the Euler equation

$$u'(c^*) = \beta \int e^{-\gamma S'} r(K', S') \cdot u'(c'^*) \cdot \underbrace{\left\{ \frac{e^{-V(k',K',S')/\alpha} \pi(\gamma)}{\int e^{-V(k',K',S')/\alpha} \pi(\gamma)\, \mathrm{d}\gamma} \right\}}_{\hat{\pi}(\gamma)} \mathrm{d}\gamma,$$

where $e^{-\gamma S'} r(K', S')$ is the realized next period per-unit capital income after considering the effect of GHG-induced deterioration. Weighting the expectation by $\hat{\pi}(\gamma) = \frac{e^{-V(k',K',S')/\alpha} \pi(\gamma)}{\int e^{-V(k',K',S')/\alpha} \pi(\gamma)\, \mathrm{d}\gamma}$ instead of $\pi(\gamma)$ captures the effect of model uncertainty. Moreover, on the equilibrium path, the optimal capital choice of the representative agent must be consistent with the transition law for the aggregate capital stock, that is, $\tilde{k}^*(K, K, S) = G(K, S)$. Some algebra leads to the following proposition.

PROPOSITION 3.2. *Assume that* A1–A8 *hold. The optimal tax,* $\tau^*(K, S) = \frac{\lambda^s}{u'(C^*)} = \nu K^\theta [c_E(1 - \Delta S)]^{\nu - 1}$, *rebated as a lump-sum payment, leads to a competitive equilibrium allocation that coincides with the solution to the planner's problem. That is, the equilibrium energy/emissions are* $E^* = c_E(1 - \Delta S)$ *and the equilibrium consumption is given by* $c^* = C^* = (1 - \beta\theta) K^\theta [c_E(1 - \Delta S)]^\nu$.

4. CALIBRATION AND THE COMPUTATIONAL SOLUTION

To investigate the implications of model uncertainty for optimality and for environmental policy, we will develop and calibrate a generalized version of the model studied in the previous section. While the theoretical model remains instructive, the calibrated model illustrates two distinct results from GHKT. First, the concern about model uncertainty causes a significant decline in the use of coal. In contrast, the use of oil/gas is delayed, but eventually oil/gas reserves are exhausted. Second, similar to the analytical results of the benchmark model, but unlike in GHKT, the level of GHG concentration affects the optimal tax rate.

We will calibrate the model after (i) relaxing assumption A5 and allowing the labor productivity (or the population) to grow at an exogenous rate g, which we calibrate to be 2 percent per year, (ii) relaxing assumptions A6.1 and A6.2, which will allow for the dynamics of the GHG concentration to mimic GHKT's environmental model, (iii) relaxing assumption A7 and incorporating a "coal" and a "green" sector into the model, and (iv) relaxing assumption A8 so as to study the effect of a finite supply of oil/gas.

To solve (2) under assumptions A1–A4 and with labor productivity given by $A_N = 1 + g$, we will make use of the analysis in the previous section. The main difference is that the function $f(\cdot)$, defined as in (5), is now a function of labor productivity, the permanent and temporary parts of the GHG concentration, and the remaining reserves of oil/gas. Moreover, $f(\cdot)$ no longer has a closed-form expression. We will again apply the

outer- and inner-loop method used in Section 3. The inner-loop minimization problem is unchanged, while the outer-loop maximization problem will be solved in parts. It is useful to note that solving the optimization problem for E_i, P', T', and R' can be carried out separately from solving for $C^* = (1-\beta\theta)Y^*$ and $\tilde{K}'^* = \beta\theta Y^*$, where Y^* denotes the optimal output level. After substituting for C^*, the optimization problem for E_i, P', T', and R' can be simplified, leading to the dynamic programming problem

$$f(N,P,T,R) = \max_{E_1,E_2,E_3}\left\{\frac{1}{1-\beta\theta}\log\left[\left(1-\frac{E_2}{A_2N}-\frac{E_3}{A_3N}\right)^{1-\theta-\nu}E^{\nu}\right] + \beta\left[f\left(N',P',T',R'\right)+\alpha\log\left(1-\Delta S'\right)\right]\right\}, \tag{14}$$

s.t.

$$E = \left(\kappa_1 E_1^{\rho}+\kappa_2 E_2^{\rho}+\kappa_3 E_3^{\rho}\right)^{1/\rho},$$
$$N' = (1+g)N,$$
$$R' = R - E_1 \geq 0,$$
$$P' = P + \phi_L(E_1+E_2),$$
$$T' = (1-\phi)T + (1-\phi_L)\phi_0(E_1+E_2),$$
$$S' = P' + T'.$$

The marginal value of the externality from GHG as a fraction of output, denoted by $\hat{\Lambda}^S$, can be defined as follows.[14] Increasing E_1+E_2 by one unit is equivalent to simultaneously increasing P by ϕ_L units and T by $\frac{(1-\phi_L)\phi_0}{1-\phi}$ units. Therefore, $\hat{\Lambda}^S$ is given by

$$\hat{\Lambda}^S = \phi_L\hat{\Lambda}^P + \frac{(1-\phi_L)\phi_0}{1-\phi}\hat{\Lambda}^T, \tag{15}$$

where $\hat{\Lambda}^P = -(1-\beta\theta)\frac{\partial f}{\partial P}$ and $\hat{\Lambda}^T = -(1-\beta\theta)\frac{\partial f}{\partial T}$ give the marginal value of the externality caused by P and T, respectively. Applying the envelope theorem to the choice of P and T in (14) yields

$$\frac{\partial f}{\partial P} = \beta\left(\frac{\partial f}{\partial P'}-\frac{\alpha\Delta}{1-\Delta S'}\right), \tag{16}$$

$$\frac{\partial f}{\partial T} = \beta(1-\phi)\left(\frac{\partial f}{\partial T'}-\frac{\alpha\Delta}{1-\Delta S'}\right). \tag{17}$$

[14] If we denote the marginal value of the externality measured in units of utility by λ, then $\Lambda = \frac{\lambda}{u'(c)}$ would be the marginal value of the externality in terms of output, which is equal to the optimal tax, $\tau^* = \Lambda$. Then $\hat{\Lambda} = \frac{\Lambda}{Y}$ represents the marginal value of the externality proportional to output.

Using equations (16) and (17) and restoring the time index, t, we calculate the marginal values of the externalities associated with P and T to be

$$\hat{\Lambda}_t^P = \theta\bar{\gamma}\sum_{j=1}^{+\infty}\frac{\beta^j}{1-\Delta S_{t+j}}, \tag{18}$$

$$\hat{\Lambda}_t^T = \theta\bar{\gamma}\sum_{j=1}^{+\infty}\frac{\left[\beta(1-\phi)\right]^j}{1-\Delta S_{t+j}}, \tag{19}$$

where we used $(1-\beta\theta)\alpha\Delta = (1-\beta\theta)\alpha\frac{\bar{A}}{\alpha\lambda} = \theta\lambda^{-1} = \theta\bar{\gamma}$. Here, $\lambda^{-1} = \bar{\gamma}$ is the mean of γ under the exponential approximating model. Thus, from (15), the marginal externality of S can be expressed as

$$\hat{\Lambda}_t^S = \theta\bar{\gamma}\sum_{j=1}^{+\infty}\left[\phi_L\frac{\beta^j}{1-\Delta S_{t+j}} + \frac{(1-\phi_L)\phi_0}{1-\phi}\frac{\left[\beta(1-\phi)\right]^j}{1-\Delta S_{t+j}}\right]. \tag{20}$$

It is instructive to consider the case when there is no concern about model uncertainty, that is, $\alpha\to+\infty$. Since $\Delta\to 0$ as $\alpha\to+\infty$, in this case we have

$$\lim_{\alpha\to\infty}\hat{\Lambda}_t^S = \theta\beta\bar{\gamma}\left[\frac{\phi_L}{1-\beta} + \frac{(1-\phi_L)\phi_0}{1-(1-\phi)\beta}\right]. \tag{21}$$

Contrasting this equation with the corresponding equation (12) in GHKT, $\hat{\Lambda}_t^S = \bar{\gamma}[\frac{\phi_L}{1-\beta} + \frac{(1-\phi_L)\phi_0}{1-(1-\phi)\beta}]$, we can identify two differences. First, equation (21) contains an additional term, θ, because in our model, GHG directly affects aggregate capital instead of output. Second, the externality related to P and T is weighted by β in equation (21) because GHG affects the next period's, rather than the current period's, capital.

Using the marginal externalities from the different types of energy, we find that the optimal choice of E_3, E_2, and E_1 in the solution for (14) implies

$$\frac{\nu\kappa_3}{E_3^{1-\rho}E^\rho} = \frac{1-\theta-\nu}{A_3N}, \tag{22}$$

$$\frac{\nu\kappa_2}{E_2^{1-\rho}E^\rho} - \hat{\Lambda}^S = \frac{1-\theta-\nu}{A_2N}, \tag{23}$$

$$\frac{\nu\kappa_1}{E_1^{1-\rho}E^\rho} - \hat{\Lambda}^S = \beta\left[\frac{\nu\kappa_1}{\left(E_1'\right)^{1-\rho}\left(E'\right)^\rho} - \left(\hat{\Lambda}^S\right)'\right]. \tag{24}$$

Note that since the energy produced from renewable sources and that produced from coal are assumed to use labor, their optimal levels, characterized by (22) and (23), depend on the relative labor productivity in the corresponding sectors, as well as on the share of labor in the final goods production, $1-\theta-\nu$. In contrast, since oil/gas is not using labor, its optimal choice, characterized by (24), is independent of the labor productivity and share. Instead, given a limited supply of oil/gas, the optimal choice of E_1

is found by equating the marginal net benefit from using one unit of oil/gas reserves in the current period to the present value of the marginal net benefit from postponing consumption until the next period. Note that the marginal net benefits from energy coming from oil/gas and coal, given in the left-hand sides of (23) and (24), respectively, incorporate the marginal robust externality from the resulting GHG emissions, $\hat{\Lambda}^S$. Finally, note that the expectation operator, $\mathbb{E}_t$, does not appear on the right-hand side of (24). While fossil fuel use depends on the current level of GHG concentration, S, and on the expected marginal externality, it is independent of the level of capital and, thus, of the realized value of the damage parameter, γ. In this sense, the path of fossil fuel use is predetermined.

So as to compare the case in which there is concern about model uncertainty with the case where there is none, we numerically solve (14) for the cases of $\alpha = 0.01$ and $\alpha = \infty$. To make comparisons as straightforward as possible, we use the same parameter values as in GHKT, with the exception of the parameter governing the distribution of the damage function, which will be discussed below. The parameter values are reported in Table 1, and we refer the reader to GHKT for a detailed discussion. The results are reported in Figures 2 and 3.[15]

We will refer to the optimal paths under $\alpha = \infty$ as the *nonrobust optimal paths* and to those under $\alpha = 0.01$ as the *robust optimal paths*. The nonrobust paths are almost identical to GHKT, as we adjust the approximating distribution to incorporate the difference between our model and the model used by GHKT. Specifically, we assume that $\lambda^{-1} = (\beta\theta)^{-1} \cdot \bar{\gamma}_{\text{GHKT}}$, where $\bar{\gamma}_{\text{GHKT}}$ is the mean of the distribution governing the externality parameter in GHKT. Under this parametrization, the expected externality from GHG is very close across the two models.[16]

Figure 2 shows the optimal path for the use of green energy, coal, and oil/gas, as well as the resulting carbon concentration, for different levels of concern about model uncertainty.[17] Since the green energy sector does not emit carbon, the optimal path for green

TABLE 1. Calibration summary.

θ	ν	β	R_0
0.3	0.04	0.985^{10}	253.8
κ_1	κ_2	ρ	$1+g$
0.5008	0.08916	−0.058	1.02^{10}
P_0	T_0	$A_{2,0}$	$A_{3,0}$
103	699	7693	1311
ϕ	ϕ_L	ϕ_0	λ^{-1}
0.0228	0.2	0.393	2.38×10^{-5}

[15]The reported results assume that the realized value of the damage parameter, γ, is equal to its expected value, given the underlying distribution.

[16]Although GHKT employ a normal approximating distribution, while we use an exponential, both distributions yield very similar results, as we show in the next subsection.

[17]We assume throughout that the realized value of the damage parameter, γ, is equal to the mean of the distribution.

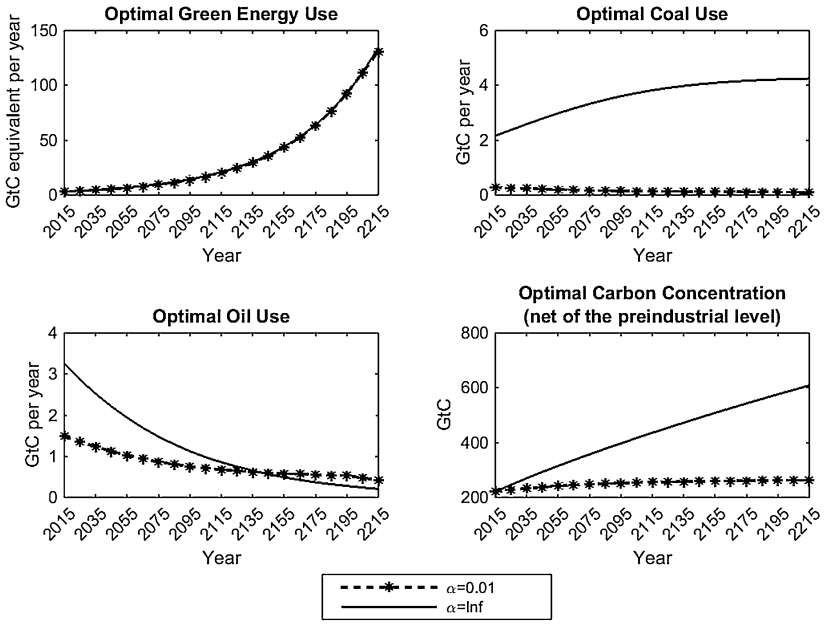

FIGURE 2. Robust and nonrobust optimal use of energy.

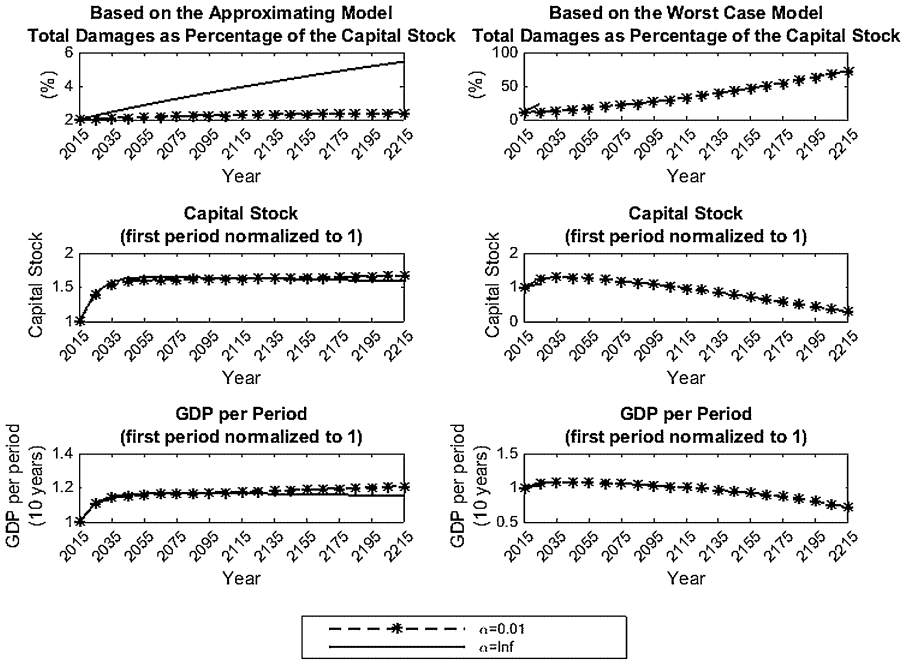

FIGURE 3. Robust and nonrobust capital stock and output.

energy use does not directly depend on the concern about model uncertainty. However, since green energy is a substitute for energy generated by coal and oil/gas, model uncertainty considerations affect the use of green energy *indirectly*. The numerical results reported on the top-left panel of Figure 2 suggest that the indirect effect on green energy use is minute.

The robust optimal use of coal is significantly lower than the nonrobust use, as the top-right panel of Figure 2 depicts. Moreover, while the nonrobust optimal path of coal use is increasing, the robust path is decreasing. This finding results from the fact that under model uncertainty, the marginal externality is dependent on the level of the GHG concentration. More formally, from (20) it follows that for $\alpha = \infty$, we have $\Delta = 0$; thus, the externality from carbon emissions, $\hat{\Lambda}^S$, is independent of the current and future levels of GHG concentration. However, as discussed in the previous section, when $\alpha < \infty$, higher GHG concentrations increase the level of the externality from carbon emissions. Thus, unlike the nonrobust optimal path, coal use declines with increasing GHG emissions along the robust optimal path.

As reported in the bottom-left panel of Figure 2, in contrast to the use of coal, the concern about model uncertainty only delays the optimal use of oil/gas. Since the supply of oil/gas is finite and binding, model uncertainty has only a small effect on the cumulative use of oil/gas. However, since under model uncertainty the externality from carbon emissions is dependent on the level of the GHG concentration, a smoother path of oil/gas use would allow for the partial absorption of the temporary part of the atmospheric GHG, T, and would thus reduce the total externality from emissions.

The concern about model uncertainty reduces the optimal GHG concentration significantly. As shown in the bottom-right panel of Figure 2, atmospheric carbon concentration on the nonrobust path continues to grow over time, as the externality from carbon emissions is not affected by the carbon concentration. However, the robust path of carbon concentration remains below the $\Delta^{-1} = \frac{(1-\beta\theta)\alpha\lambda}{\theta}$ breakout threshold.[18] This boundedness property results from the fact that a higher carbon concentration would increase the externality from carbon emissions, and thus curb the optimal emissions level. The difference between the nonrobust and robust optimal carbon concentration is quantitatively significant. The calibrated model predicts that the nonrobust carbon concentration (net of the pre-industrial level) will rise almost threefold over the course of 200 years and reach a level of 600 gigatons. In contrast, the robust optimal carbon concentration in our model will increase by less than one-third and remain well below 300 gigatons.

The effect of model uncertainty on global temperatures is substantial. To map carbon concentrations from the calibrated model into global temperatures, we use the ex-

[18]As we discussed in the previous section, if the GHG concentration $S' \geq \frac{1}{\Delta}$, then the system cannot be "robustified," in the sense that the value of the game goes to negative infinity.

pression in GHKT,[19]

$$T(S_t) = 3\ln\left(\frac{S_t}{\bar{S}}\right)\Big/\ln 2,$$

where $\bar{S}$ is the pre-industrial level of atmospheric carbon concentration.

In GHKT, the average current global temperature is calculated to be 1.4 degrees Celsius above its pre-industrial level. In the calibrated version of the model, carbon concentration in the nonrobust path implies an average global temperature increase of more than 1.6 degrees Celsius over the course of 200 years, with global temperatures reaching more than 3 degrees Celsius above the pre-industrial level. In contrast, the average global temperature in the robust path implies an increase of about 0.2 degrees Celsius.

It is worth providing some perspective on the effects from various temperature increases. The most recent Intergovernmental Panel on Climate Change (IPCC) report outlines the perceived damages from a range of temperature increases and points to the need for further rigorous assessment. According to the report, a 1-degree Celsius increase would increase the risk of extreme weather events, such as heat waves, heavy precipitation, and coastal flooding. Under a warming of above 2 degrees Celsius, the risks of affecting crop yields and water availability are perceived to be high. Risks to the global economy are judged to be moderate under an additional 1–2 degrees Celsius warming. The IPCC report emphasizes that a few quantitative estimates are available for a warming of above 3 degrees Celsius. Risks associated with tipping points are perceived to be moderate between 0 and 1 degrees Celsius, but they increase at a steepening rate under an additional 1–2 degrees of warming and are perceived to become high above 3 degrees Celsius.[20]

According to the calibrated model, the difference between the nonrobust and the robust carbon concentration paths has a noticeable effect on the real economy. The panels on the left side of Figure 3 depict how switching from the nonrobust to the robust path affects the economy's capital stock and output based on the approximating model—the decision maker's baseline model—being the true model. As before, we assume that the realized value of the damage parameter, γ, is equal to the mean of the corresponding distribution on the entire path. Due to the lower accumulation of atmospheric carbon on the robust path, the expected damage to the capital stock will be about 3 percentage points lower and will remain below 3 percent of the capital stock after 200 years. However, the increased damages do not have a significant effect on the capital stock or on output, because the lower carbon emissions on the robust path are achieved by a significant cut in the use of coal and, thus, a lower energy input used in the production of the final good. In fact, for the first 100 years, output is lower on the robust path and only surpasses the robust path toward the end of the reported 200 years.

[19]GHKT argue that the reduced-form composition mapping from carbon concentrations to temperature increases and then to damages that they employ, is a reasonable approximation to the one calibrated by Nordhaus (Figure 1 in GHKT). So as to identify the effects from introducing model uncertainty as cleanly as possible, we keep the other aspects of their modeling, including the damage formula, initial temperature, and so forth, intact.

[20]See IPCC (2014).

The panels on the right-hand side of Figure 3 depict how switching from the nonrobust to the robust path affects capital stock and output, assuming that the true distribution of the damage parameter, γ, evolves according to the worst-case model in each period. Again, we assume that the realized value of γ is equal to the mean of the corresponding distribution. The carbon concentration on the nonrobust path surpasses the breakout threshold after 20 years (see the bottom-right panel of Figure 2). Even on the robust path, the carbon concentration gets very close to the breakout threshold. Thus, the expected damages according to the worst-case model rise to as high as 70 percent of the capital stock over 200 years. Note that the worst-case distribution depends on the level of the GHG concentration. Therefore, as carbon concentrations increase, the mean of the distribution of the damage parameter, which is assumed to be the realized value of γ on the reported path, rises. The resulting sharp decline in capital stock and on output are reported in the two bottom-right panels in Figure 3. The dramatic effects of the worst-case model on capital stock and on output are the reason for the sharp cut in the use of coal on the robust path, as reported in the top-right panel of Figure 2. These effects are partly magnified by the assumption that the approximating distribution of the damage parameter is exponential. As we discuss next, the losses are somewhat reduced, though still large, if the approximating distribution is assumed to be normal.[21]

4.1 *Robust optimal taxation*

As we showed in the benchmark model, the robust optimal allocation can be implemented by imposing a tax on carbon emissions and rebating the proceeds to the agents. The same type of tax/rebate can implement the optimal allocation in the general case. As depicted in the top panel of Figure 4, a higher concern about model uncertainty results in a higher carbon tax. Specifically, the optimal tax rate for the "robust" path discussed earlier ($\alpha = 0.01$) would surpass more than 25 times the optimal tax in the nonrobust path, in which there is no concern about model uncertainty ($\alpha = \infty$). Moreover, unlike the nonrobust optimal tax, which remains constant over time, the robust optimal tax is *increasing* over time. Note that, as discussed in the benchmark model, the optimal tax rate depends on the level of consumption or, equivalently, on output; that is, $\tau^* = \frac{\lambda}{u'(C)}$. To abstract from the increase in the carbon tax rate that is the result of economic growth, we are reporting the tax rate in terms of the output in the starting year, \$70 trillion.[22]

The rise of the robust optimal carbon tax rate is due to the externality from increased GHG concentrations. As we showed in the analytical solution for the benchmark model, a deviation from the approximating distribution is more attractive for the malevolent player when the GHG concentration is higher. The externality from carbon emissions is

[21] Stern (2013) has criticized existing estimates of costs associated with climate change for not taking into consideration nonnegligible probabilities of catastrophic events. As the exponential distribution is "fat tailed," it implies a higher probability of extreme values than, say, a normal distribution.

[22] Formally, Figure 4 reports $\hat{\Lambda}_t^S \times Y_{2015}$, where $\hat{\Lambda}^S$ is the marginal externality proportional to output, while the robust optimal tax rate should be $\tau_t^* = \Lambda_t^S = \hat{\Lambda}_t^S \times Y_t$.

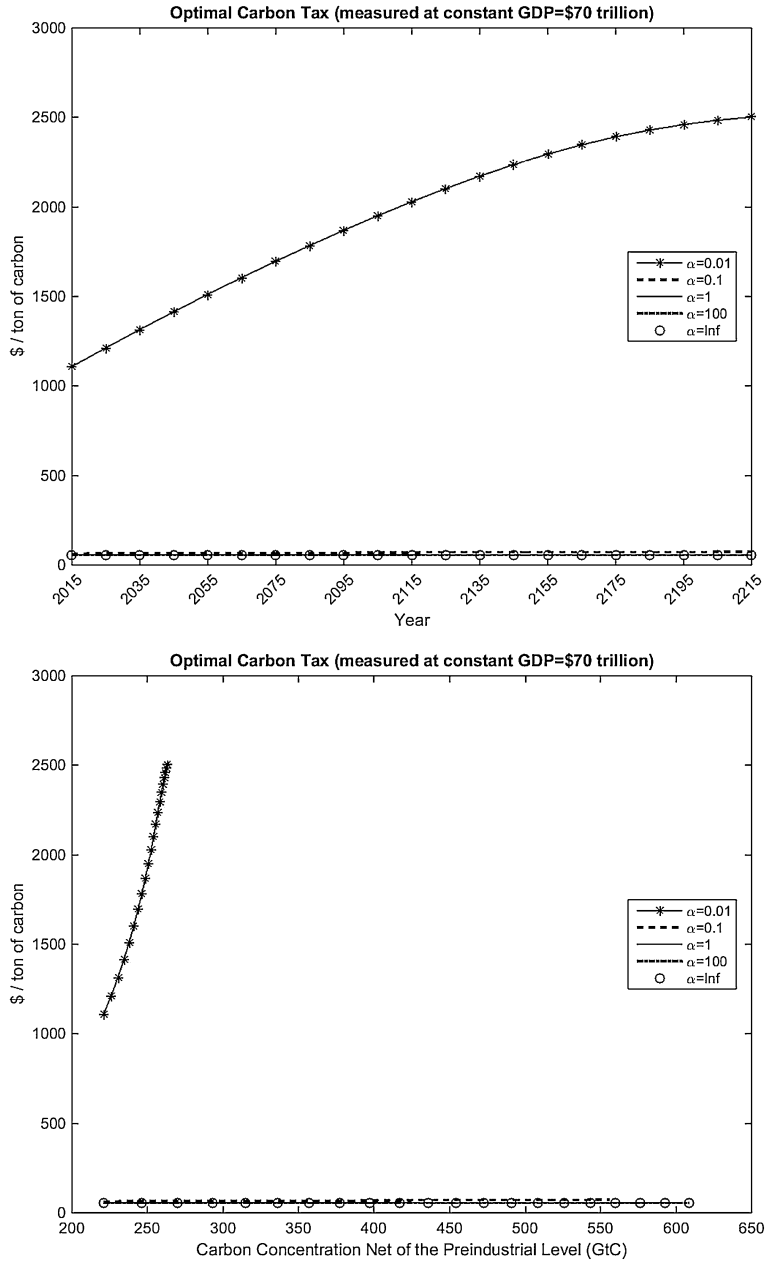

FIGURE 4. Robust optimal taxation.

larger for higher GHG concentrations due to the concern about the malevolent player's reaction. The interaction between the concern about model uncertainty and the GHG concentrations is depicted in the bottom panel of Figure 4.[23] A higher concern about

[23]The permanent and the transitory components of the GHG concentration are associated with different externalities, as shown in (18) and (19). Thus, the robust optimal tax rates for the same levels of total GHG

model uncertainty (lower α) not only results in a higher level of carbon tax rate per unit of output, but also makes the rise of the tax rate on GHG concentrations steeper. To curb consumption of fossil fuel as the GHG concentration gets closer to the breakout threshold, the robust optimal tax rate must rise. Thus, a higher concern about model uncertainty results in a steeper tax rise.

4.2 *An alternative approximating distribution*

In this section we explore the sensitivity of our results to assumption A3, regarding the approximating distribution of the damage function parameter, γ. More precisely, we will replace the exponential approximating distribution and assume instead that the approximating distribution of γ is normal with mean $\bar{\gamma}$ and variance σ^2; that is, $\pi(\gamma) = \frac{1}{\sqrt{2\pi\sigma^2}} e^{-(\gamma-\bar{\gamma})^2/(2\sigma^2)}$. As we will show, this change has some implications for the worst-case models and, therefore, for the breakout threshold. However, the quantitative implications from switching to a normal distribution are more subtle.

Using a normal distribution to approximate γ eliminates the breakout threshold. Unlike the exponential distribution, which is characterized by a single parameter, λ, the normal distribution has 2 degrees of freedom: its mean, $\bar{\gamma}$, and its variance, σ^2. As the exponential distribution has a "fat tail," a larger mean implies a higher variance, which in turn makes it harder for the system to be robustified. In contrast, under a normal distribution, the malevolent player's alteration of the distribution would affect only the mean of the approximating distribution, and the worst-case distribution would have the same variance. Thus, there is no breakout threshold for the mean above which the system cannot be robustified.

More formally, using a normal approximating distribution for the penalty parameter, α, the worst-case distribution will be given by

$$\hat{\pi}^*(\gamma) \sim \mathcal{N}\left(\bar{\gamma} + \frac{\bar{A}\sigma^2}{\alpha} S'^2, \sigma^2\right),$$

while the robust externality is given by

$$H(S'; \alpha, \bar{A}) = -\left(\bar{\gamma} + \frac{\bar{A}\sigma^2}{2\alpha} S'\right) \bar{A} S'. \tag{25}$$

Recall that the externality under an exponential distribution was given by (8). This equation can be written as $H(S'; \alpha, \bar{A}) = \alpha \log(1 - \frac{\bar{\gamma}\bar{A}}{\alpha} S')$, which is unbounded for $S' \geq \frac{1}{\Delta} = \frac{\alpha}{\bar{\gamma}\bar{A}}$. In contrast, there is no threshold for S' after which the externality under the normal distribution, given by (25), becomes unbounded.

A change in $H(\cdot)$ would also change the externality associated with the GHG concentration. In particular, by replacing the term $\alpha \log(1 - \Delta S')$ in equation (14) with

concentrations, but a different composition of permanent and transitory parts, are different. The horizontal axis in Figure 4 reports the total GHG concentrations over the robust path for different levels of concern about model uncertainty.

$-(\bar{\gamma}+\frac{\bar{A}\sigma^2}{2\alpha}S')\bar{A}S'$, we would have

$$\hat{\Lambda}_t^P=\frac{\beta\theta\bar{\gamma}}{1-\beta}+\frac{\theta\bar{A}\sigma^2}{\alpha}\sum_{j=1}^{+\infty}\beta^j S_{t+j},$$

$$\hat{\Lambda}_t^T=\frac{\beta(1-\phi)\theta\bar{\gamma}}{1-\beta(1-\phi)}+\frac{\theta\bar{A}\sigma^2}{\alpha}\sum_{j=1}^{+\infty}\big[\beta(1-\phi)\big]^j S_{t+j}.$$

This expression, in turn, implies

$$\begin{aligned}\hat{\Lambda}_t^S&=\phi_L\hat{\Lambda}_t^P+\frac{(1-\phi_L)\phi_0}{1-\phi}\hat{\Lambda}_t^T\\&=\beta\theta\bar{\gamma}\left\{\frac{\phi_L}{1-\beta}+\frac{(1-\phi_L)\phi_0}{1-\beta(1-\phi)}\right\}\\&\quad+\frac{\theta\bar{A}\sigma^2}{\alpha}\sum_{j=1}^{+\infty}\big\{\phi_L+(1-\phi_L)(1-\phi)^{j-1}\phi_0\big\}\beta^j S_{t+j}.\end{aligned}\tag{26}$$

As in the exponential case, if the concern about model uncertainty goes to zero ($\alpha\to\infty$) or, alternatively, if the approximating distribution collapses to a single point ($\sigma^2\to 0$), we would have, similar to (21) in the exponential distribution case,

$$\hat{\Lambda}_t^S=\theta\beta\bar{\gamma}\left[\frac{\phi_L}{1-\beta}+\frac{(1-\phi_L)\phi_0}{1-(1-\phi)\beta}\right].$$

Given (26), the optimal mixture of renewable, coal, and oil/gas use—namely E_3, E_2, and E_1—follows (22)–(24), as before.

Figure 5 reports the robust and the nonrobust optimal path for different types of energy use, as well as the resulting carbon concentration paths under a normal approximating distribution with the same mean and variance as the exponential distribution used previously. By construction, the nonrobust paths are identical to the nonrobust paths of Figure 2. Comparing the top-left panels of Figures 2 and 5 shows that switching from an exponential distribution to an equivalent normal distribution would leave the robust optimal green energy use intact. However, the robust optimal use of coal is larger under the normal distribution. Yet, the use of coal remains slightly decreasing and significantly below the nonrobust use of coal, as shown in the top-right panel of Figure 5. Under a normal approximating distribution, the robust optimal oil/gas use would be higher and would decline faster over time compared with the exponential distribution case. Thus, as depicted in the bottom-left panel of Figure 5, the effect of switching from a nonrobust to a robust optimal path will be less significant under the normal distribution. Finally, as shown in the bottom-right panel of Figure 5, unlike in the exponential case, in which it was bounded below 300 gigatons, the robust path of carbon concentration surpasses 300 gigatons in less than 100 years. The higher carbon concentration is mainly due to a higher use of coal under the normal distribution.[24]

[24]A higher GHG concentration translates to an increase of about 0.4 degrees Celsius in the average global temperature over the course of 200 years relative to the robust path under an exponential distribution. Thus,

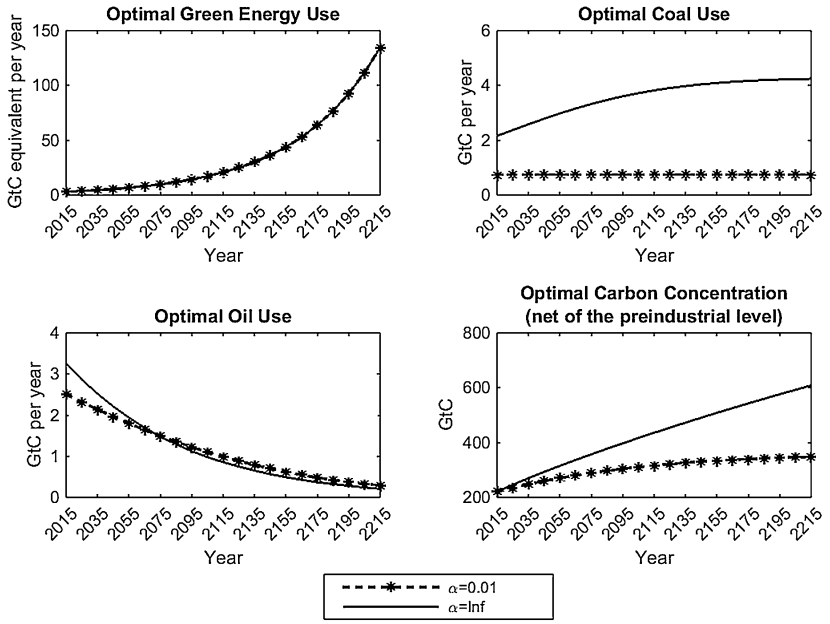

FIGURE 5. Robust and nonrobust optimal use of energy with normal approximating distribution.

The difference between the robust paths under the two alternative distributions is due to two reasons. First, as we discussed previously, there is no breakout threshold under the normal distribution. Thus, carbon emissions are not cut dramatically as the GHG concentration approaches a threshold. Second, although we use the same value for the penalty parameter ($\alpha = 0.01$) in both cases, the effects on the choice of the worst-case distribution are different. Specifically, the resulting distances between the approximating distributions, π, and those chosen by the malevolent player, $\hat{\pi}$, as measured by relative entropy are different across the two cases. Everything else being equal, the choice by the malevolent player is further apart from the approximating distribution in the exponential case. In addition, robust optimal carbon emissions are more conservative relative to the normal distribution case. It is also worth noting that the difference between the robust paths under the two alternative distributions is significantly smaller than the difference between the nonrobust paths.

Under a normal approximating distribution, the system can be robustified for any level of carbon concentration. Therefore, unlike the exponential case, the nonrobust paths based on the worst-case model are well defined, as reported in the right-side panels of Figure 6. Moreover, the difference between the robust paths of the capital stock and of output based on the approximating distribution (left-side panels of Figure 6) are not significant. However, while the corresponding robust and nonrobust paths based on the worst-case distribution (right-side panels of Figure 6) are not significantly different

under a normal approximating distribution, temperatures on the robust path are 2 degrees Celsius above the pre-industrial level.

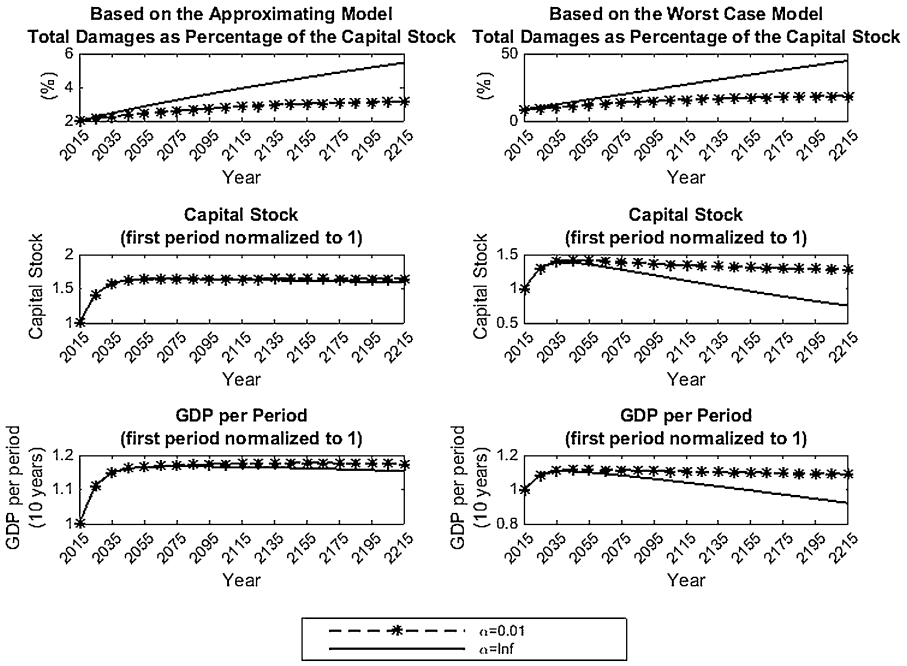

FIGURE 6. Robust and nonrobust capital stock and output with normal approximating distribution.

in early years, the differences rise to 50 percent of the output and capital stock within 200 years.

Finally, the robust path of total damages based on the approximating model is less than 1 percentage point higher under the normal approximating distribution compared with the exponential distribution, as reported on the top-left panels of Figure 6 and Figure 3. The subtle difference is due to the relatively small difference between the robust paths of carbon concentration, which are reported in the bottom-right panels of Figure 2 and Figure 5.[25]

4.3 *The stock of fossil fuel*

The supply of both oil/gas and coal are finite. For comparison, we would like to discuss the more realistic case, where there is a finite supply of coal. At the same time, advancements in unconventional oil/gas (and the future potential from offshore unconventional, methane hydrates, etc.) imply that the future supply of oil/gas is likely to be significantly larger than the one considered in GHKT.

While the concern about model uncertainty seems to affect the optimal use of coal significantly, it appears to have a limited effect on the consumption of oil/gas. This observation is at least partly due to our combined assumptions of an unbounded supply of

[25]The difference in carbon emissions and in output levels across the alternative distributions corresponds to the difference between the corresponding optimal tax policies, which is not reported for brevity.

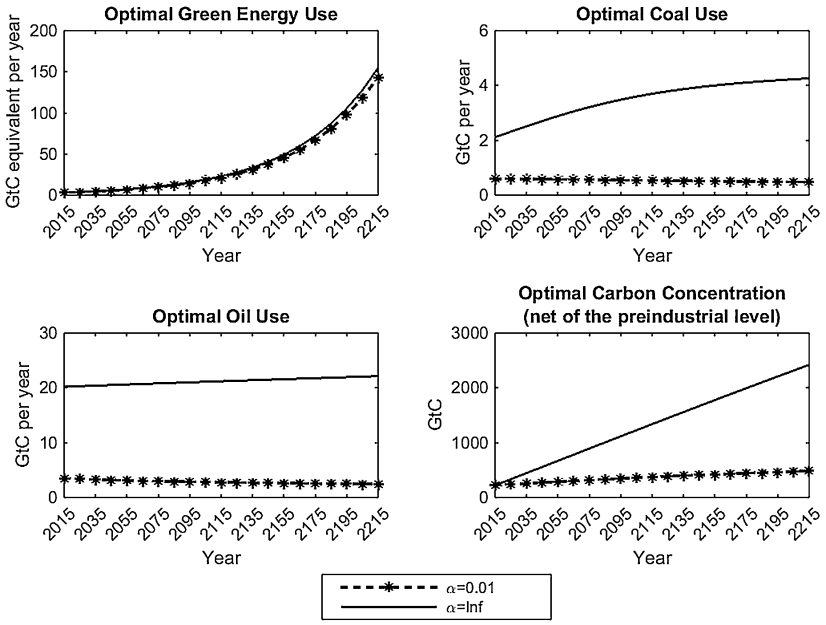

FIGURE 7. Robust and nonrobust optimal use of energy with unlimited oil/gas.

coal and a strictly binding supply of oil/gas. In this subsection, we will briefly study the implications of modifying these assumptions.

Figure 7 reports the robust and the nonrobust optimal paths for the consumption of different types of energy, as well as the resulting carbon concentrations, for the benchmark case when the supply of oil/gas is unlimited. As the economy grows, so does the nonrobust optimal use of oil/gas. This growth is similar to the growth in the nonrobust use of coal. In contrast, the robust optimal consumption path for oil/gas is bounded and decreasing because the rising GHG concentration increases the externality from carbon emissions, thus curbing the use of oil/gas. Interestingly, even the use of green energy is eventually lower on the robust optimal path. Since the GHG concentration is higher on the nonrobust path, the capital stock will eventually be lower on the nonrobust path. In turn, the lower capital input in the final goods production leads to the allocation of extra resources in the production of all types of energy, including green energy.

Figure 8 reports both the robust and the nonrobust paths when the supply of oil/gas and that of coal are limited, and it compares these with the benchmark case of an unlimited supply of coal. More precisely, we assume that the initial stock of oil/gas is given by 253.8 GtC (the GHKT benchmark), while the initial stock of coal is given by $R_{\text{coal}} = 666$.[26] While adopting this more realistic assumption about the stock of coal does not appear to have a noticeable effect on the robust optimal use of different types of energy, it has a significant effect on the optimal nonrobust use of coal and, thus, on carbon concentrations. Nevertheless, the assumption that the stock of coal is limited is not sufficient to

[26]The total stock of coal is obtained by applying the conversion factors provided by the U.S. Energy Information Administration to the estimated resources of coal as reported by the U.S. Geological Survey. This calculation leads to 2441 gigatons (Gt) of CO_2 or, applying the 12/44 conversion, to 665.7272 GtC.

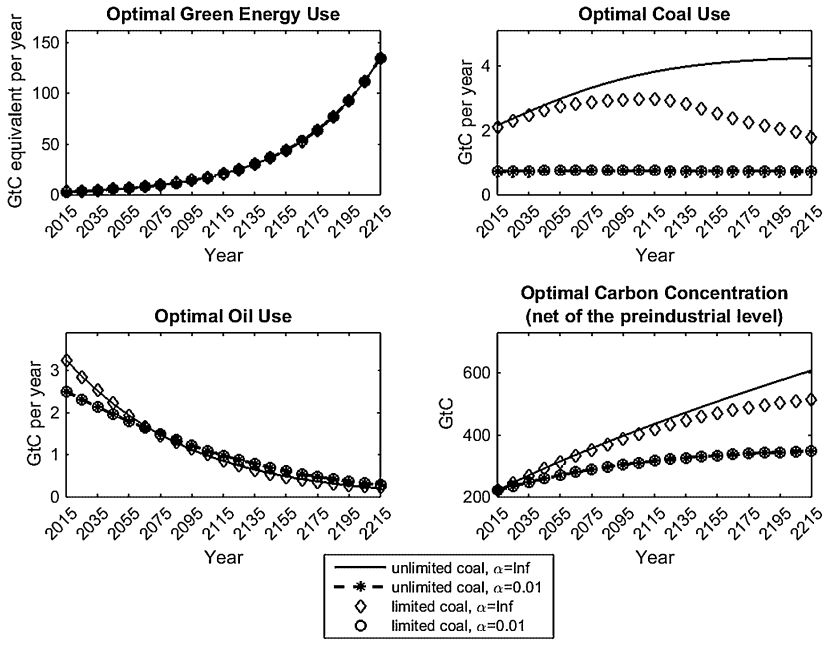

FIGURE 8. Effect of coal on robust and nonrobust optimal use of energy.

bring the nonrobust use of coal in line with its robust use. In short, the concern about robustness matters for the optimal consumption of coal, even when its supply is limited.

5. CONCLUSION

We studied optimal taxation and the resulting optimal energy mix in a dynamic stochastic general equilibrium model in which agents are concerned about model uncertainty regarding damages resulting from climate change. We used robust control to model the optimal response to this uncertainty by optimizing agents. We demonstrated that Pigouvian taxation restores the socially optimal allocation. This is in sharp contrast to existing policies around the world, which subsidize fossil fuel. We showed that the concern about model uncertainty causes a significant decline in the optimal use of coal, and a smoother path of oil/gas consumption. Interestingly, the concern about model uncertainty does not have a noticeable effect on the optimal path of green energy use. Moreover, we show how the concern about model uncertainty yields a robust optimal Pigouvian tax, under which the excessive damages of the worst-case scenarios are avoided.

Our work built heavily on the model introduced in GHKT. While admittedly restrictive, this framework allowed us to derive an analytical solution for the benchmark case and to develop a recursive method to solve the model computationally under more general assumptions. As in GHKT, we concluded that the use of coal should be constrained. Furthermore, we showed that the concern about model uncertainty results in a significant additional decline in the robust optimal use of coal. The core theoretical result in GHKT is that, when expressed as a proportion of GDP, the optimal tax on emissions is

independent of the stochastic value of the future output and of the stock of carbon in the atmosphere. In contrast, we showed that even under the restrictive assumptions in GHKT, the robust optimal tax rises as the GHG concentration increases once we consider model uncertainty, even though the expected damages remain unchanged.

In this paper, we concentrated on the uncertainty associated with damages from carbon concentration. Of course, several other variables can be introduced and modeled as being subject to uncertainty. These variables include those governing the dynamics of carbon concentration, those governing productivity growth and, hence, future production, the labor costs and elasticities of substitution associated with different sources of energy, and the risks from nuclear energy. Studying alternative sources of uncertainty is a natural extension of our model. Similarly, we could study the effect of introducing extraction/exploration costs, as in Hartley et al. (2016). Our model can be extended in other ways. In this paper, we assume that the growth rate of renewables is independent of the concern about model uncertainty. It would be interesting to endogenize growth in renewable energy productivity as in Adao, Narajabad, and Temzelides (2012). A related extension could involve using a distortionary tax on labor to subsidize research and development in renewables and studying the resulting effects on energy composition and growth. These extensions are left to future research.

Appendix

Here we demonstrate that the optimal level of GHG, E^*, has the properties $\frac{\partial E^*}{\partial \delta} < 0$ and $\frac{\partial E^*}{\partial \delta}|_{\delta=0} = -\infty$, where δ is the upper bound for entropy allowed in the constraint game.

Proof. Recall that $E^* = c_E(1 - \Delta S)$ and $\delta = \log(1 - \Delta S'^*) + \frac{\Delta S'^*}{1-\Delta S'^*}$, where $S'^* = S + \phi_0 c_E(1 - \Delta S)$. Define $a = \alpha^{-1}$ and $b = 1 - \Delta S'^* = (1 - \Delta \phi_0 c_E)(1 - \Delta S)$. It follows immediately that E^* is decreasing in a. In addition, since both Δ and c_E are functions of a, it follows that b is a function of a:

$$b(a) = \big[1 - \Delta(a)\phi_0 c_E(a)\big]\big[1 - \Delta(a)S\big].$$

It is easy to see that b is decreasing in a. Thus, it defines a as an implicit function of b, with a negative slope. Moreover, we can rewrite δ as

$$\delta = \log b + \frac{1-b}{b},$$

which defines b as an implicit function of δ. Direct calculation shows that $\frac{\partial b}{\partial \delta} = -\frac{b^2}{1-b} < 0$, as $b \in (0, 1)$. Thus,

$$\frac{\partial E^*}{\partial \delta} = \frac{\partial E^*}{\partial a}\frac{\partial a}{\partial b}\frac{\partial b}{\partial \delta} < 0.$$

Evaluating this expression at $\delta = 0$, we obtain

$$\left.\frac{\partial E^*}{\partial \delta}\right|_{\delta=0} = \left(\left.\frac{\partial E^*}{\partial a}\right|_{a=0}\right)\left(\left.\frac{\partial a}{\partial b}\right|_{b=1}\right)\left(\left.\frac{\partial b}{\partial \delta}\right|_{\delta=0}\right).$$

It is straightforward to show that the first two terms on the right-hand side in the previous expression are strictly negative and finite, while the last term goes to $-\infty$. Therefore, $\frac{\partial E^*}{\partial \delta}|_{\delta=0} = -\infty$. □

A.1 *Equivalence between the recursive game and the date-0 game*

Here we discuss the equivalence between the recursive Stackelberg game and its date-0 counterpart. We concentrate on the one-sector model. In the recursive version of the Stackelberg game, the worst-case model for γ_{t+1} depends on the endogenous state, S_t, and on the choice variable, E_t. This feature can be difficult to interpret.[27] Alternatively, we can construct a date-0 Stackelberg game in which the malevolent player, as the leader of the game, chooses first the distorted models of $\{\gamma_{t+1}\}$, $\{\hat{\pi}(\gamma_{t+1})\}$. This choice leads to $\{\hat{\pi}(\gamma_{t+1})\}$ being independent of the endogenous states. We then show that, on the equilibrium path, the worst-case models derived from the date-0 Stackelberg game coincide with those derived from the recursive game. We demonstrate the equivalence by using the "big K–little k" result from Chapter 7 in Hansen and Sargent (2008).

Consider the Stackelberg game in which, at date-0, the minimizing player chooses the distorted probability process $\{\hat{\pi}(\gamma_{t+1})\}$, followed by the maximizing player choosing the control process $\{u_t = (C_t, E_t)\}$:

$$\inf_{m\in\mathcal{M}} \sup_{u\in\mathcal{U}} E\left[\sum_{t=0}^{\infty} \beta^t M_t\big(u(C_t) + \beta\alpha m_{t+1}\log m_{t+1}\big)\Big| S_0, K_0\right], \tag{27}$$

s.t.

$$M_{t+1} = M_t m_{t+1},$$

$$S_{t+1} = S_t + \phi_0 E_t, \tag{28}$$

$$K_{t+1} = h(S_{t+1}, \gamma_{t+1})\big[F(K_t, E_t) - C_t\big], \tag{29}$$

where $\mathcal{U}$ denotes the space of control processes $u = \{u_t : t = 0, 1, \ldots\}$ and $\mathcal{M}$ denotes the space of likelihood ratio processes $m = \{m_{t+1} = \frac{\hat{\pi}(\gamma_{t+1})}{\pi(\gamma_{t+1})} : t = 0, 1, \ldots\}$.

We introduce an exogenous state vector process $\{(\hat{S}_t, \hat{K}_t)\}$, which evolves as

$$\hat{S}_{t+1} = \hat{S}_t + \phi_0 \hat{E}_t(\hat{S}_t), \tag{30}$$

$$\hat{K}_{t+1} = h(\hat{S}_{t+1}, \gamma_{t+1})\big[F\big(\hat{K}_t, \hat{E}_t(\hat{S}_t)\big) - \hat{C}_t(\hat{S}_t, \hat{K}_t)\big], \tag{31}$$

where $\hat{E}_t(\hat{S}_t) = c_E(1 - \Delta\hat{S}_t)$ and $\hat{C}_t(\hat{S}_t, \hat{K}_t) = (1 - \beta\theta)\hat{K}_t^{\theta}[\hat{E}_t(\hat{S}_t)]^{\nu}$.[28] Note that $\{\hat{S}_t, \hat{K}_t, \hat{E}_t, \hat{C}_t\}$ are independent of the control variables $\{E_t, C_t\}$. Moreover, we set $(S_0, K_0) = (\hat{S}_0, \hat{K}_0)$.

[27] We thank Lars Hansen for bringing this point to our attention and for suggesting the use of the big K–little k result as a way to bypass the difficulty.

[28] The exogenous processes $\hat{E}_t(\hat{S}_t)$ and $\hat{C}_t(\hat{S}_t, \hat{K}_t)$ are constructed to mimic the optimal controls $E_t^*(S_t)$ and $C_t^*(S_t, K_t)$ by replacing the endogenous state (S_t, K_t) by the exogenous state $(\hat{S}_t, \hat{K}_t)$.

Define the distorted process $\{\gamma_{t+1}\}$ by

$$\gamma_{t+1} \sim \hat{\pi}(\gamma_{t+1}) = \hat{\lambda}(\hat{S}_t) e^{-\hat{\lambda}(\hat{S}_t)\gamma_{t+1}}, \tag{32}$$

where the distorted parameter, $\hat{\lambda}$, is given by $\hat{\lambda}(\hat{S}_t) = \lambda(1-\Delta\hat{S}_{t+1}) = \lambda(1-\phi_0 c_E)(1-\Delta\hat{S}_t)$. Clearly, u_t does not affect $\hat{S}_{t+1}$ and, thus, the distorted distribution $\hat{\pi}(\gamma_{t+1})$.

Given the previous exogenous distorted process, the maximizing player chooses $\{u_t\}$ at date zero to maximize the social welfare given in equation (27). With the aid of the exogenous state, this maximization problem can be expressed in a recursive form as

$$\begin{aligned}\tilde{V}(S_t, K_t, \hat{S}_t, \hat{K}_t) = \max_{C_t, E_t} \Bigg\{ & u(C_t) + \alpha\beta \int \hat{\pi}(\gamma_{t+1}) \log m_{t+1} \, \mathrm{d}\gamma_{t+1} \\ & + \beta \int \tilde{V}(S_{t+1}, K_{t+1}, \hat{S}_{t+1}, \hat{K}_{t+1}) \hat{\pi}(\gamma_{t+1}) \, \mathrm{d}\gamma_{t+1} \Bigg\},\end{aligned}$$

subject to (28), (29), (30), and (31). As shown in the main text, the relative entropy $\int \hat{\pi}(\gamma_{t+1}) \log m_{t+1} \, \mathrm{d}\gamma_{t+1}$ equals $\log(\frac{\hat{\lambda}(\hat{S}_t)}{\lambda}) + \frac{\lambda - \hat{\lambda}(\hat{S}_t)}{\hat{\lambda}(\hat{S}_t)}$. Since $\tilde{V}(\cdot)$ depends on $(\hat{S}_t, \hat{K}_t)$ only through $\hat{\pi}(\gamma_{t+1})$ or, equivalently, $\hat{\lambda}(\hat{S}_t)$, the exogenous state, $\hat{K}_t$, is eliminated from $\tilde{V}(\cdot)$. Consequently, the aforementioned problem can be rewritten as

$$\begin{aligned}\tilde{V}(S_t, K_t, \hat{S}_t) = \max_{C_t, E_t} \Bigg\{ & u(C_t) + \alpha\beta \left[\log\left(\frac{\hat{\lambda}(\hat{S}_t)}{\lambda} \right) + \frac{\lambda - \hat{\lambda}(\hat{S}_t)}{\hat{\lambda}(\hat{S}_t)} \right] \\ & + \beta \int \tilde{V}(S_{t+1}, K_{t+1}, \hat{S}_{t+1}) \hat{\pi}(\gamma_{t+1}) \, \mathrm{d}\gamma_{t+1} \Bigg\},\end{aligned}$$

subject to (28), (29), (30), and (31).

We proceed to find the solution to this date-0 problem, given the distorted process $\{\gamma_{t+1}\}$ in equation (32). Then we will argue that this solution is identical to the Markov perfect equilibrium of the sequential game defined in the main text. We implement a guess-and-verify method. We first guess that $\tilde{V}(\cdot)$ takes the form

$$\tilde{V}(S_t, K_t, \hat{S}_t) = f(S_t, \hat{S}_t) + \tilde{A} \log(K_t) + \tilde{D},$$

where $\tilde{A}$ and $\tilde{D}$ are undetermined coefficients. The functional form for $f(\cdot)$ will be derived later. Using the analysis above and the simplifications in the main text, we can write the problem as

$$\begin{aligned}& f(S_t, \hat{S}_t) + \tilde{A} \log(K_t) + \tilde{D} \\ & \quad = \max_{C_t, E_t} \Bigg\{ \log(C_t) + \alpha\beta \left[\log\left(\frac{\hat{\lambda}(\hat{S}_t)}{\lambda} \right) + \frac{\lambda - \hat{\lambda}(\hat{S}_t)}{\hat{\lambda}(\hat{S}_t)} \right] \\ & \qquad + \beta \left[f(S_{t+1}, \hat{S}_{t+1}) + \tilde{A} \log\big(F(K_t, E_t) - C_t\big) + \tilde{D} - \frac{\tilde{A} S_{t+1}}{\hat{\lambda}(\hat{S}_t)} \right] \Bigg\},\end{aligned}$$

subject to (28) and (30). Furthermore, we guess that $f(\cdot)$ takes the form $\tilde{B} \log(1-\Delta\hat{S}_t) + \frac{\tilde{G} S_t}{1-\Delta\hat{S}_t}$, where $\tilde{B}$ and $\tilde{G}$ are undetermined coefficients. After some tedious derivations, we

obtain

$$\tilde{A} = \frac{\theta}{1-\beta\theta}, \tag{33}$$

$$\tilde{G} = \frac{\beta\theta}{(1-\beta\theta)\lambda(\beta-1+\Delta\phi_0 c_E)} \tag{34}$$

and

$$E_t^{\text{opt}} = \frac{\nu(1-\Delta\hat{S}_{t+1})}{(1-\beta\theta)\beta\phi_0\left(\dfrac{\theta}{(1-\beta\theta)\lambda}-\tilde{G}\right)} = c_E(1-\Delta\hat{S}_t), \tag{35}$$

$$C_t^{\text{opt}} = \frac{F(K_t,E_t)}{1+\beta\tilde{A}} = (1-\beta\theta)K_t^{\theta}\big(E_t^{\text{opt}}\big)^{\nu}. \tag{36}$$

When $(S_0,K_0)=(\hat{S}_0,\hat{K}_0)$, we obtain $E_t^{\text{opt}}=\hat{E}_t(\hat{S}_t)=E_t^*(S_t)$, $C_t^{\text{opt}}=\hat{C}_t(\hat{S}_t,\hat{K}_t)=C_t^*(S_t,K_t)$, $\hat{S}_{t+1}=S_{t+1}$, and $\hat{K}_{t+1}=K_{t+1}$, for $t=0,1,\ldots$. In addition, $\hat{\pi}(\gamma_{t+1})=\hat{\lambda}(\hat{S}_t)e^{-\hat{\lambda}(\hat{S}_t)\gamma_{t+1}}$, where $\hat{\lambda}(\hat{S}_t)=\lambda(1-\phi_0c_E)(1-\Delta\hat{S}_t)=\lambda(1-\phi_0c_E)(1-\Delta S_t)$. That is, the optimal choices in the date-0 game coincide with the Markov perfect equilibrium allocation in the recursive game.

A.2 *The numerical solution*

Here we provide a brief description of our numerical procedure for both the normal distribution and the exponential distribution case regarding the parameter γ. Replication files are available in a supplementary file on the journal website, http://qeconomics.org/supp/463/code_and_data.zip.

A.2.1 *Normal distribution of* γ Assume (i) 100 percent capital depreciation, (ii) a Cobb–Douglas production function, and (iii) an exponential damage function. From the analysis in Sections 3 and 4, it follows that the value function takes the form

$$V(K,N,P,T,R) = f(N,P,T,R) + \bar{A}\log(K) + \bar{D},$$

where $\bar{A}=\frac{\theta}{1-\beta\theta}$ and $\bar{D}$ is a constant. The inner-loop minimization problem for $\hat{\pi}(\gamma)$ remains the same as in the one-sector model in Section 3. Furthermore, the outer-loop maximization problem for E_i, P', T', and R' can be carried out separately from the optimization problem for C and $\tilde{K}'$. The solution to the latter also remains the same as in Section 3; that is, $C^*=(1-\beta\theta)Y^*$ and $\tilde{K}'^*=\beta\theta Y^*$, where Y^* denotes the optimal output level. After substituting for C^*, the optimization problem for E_i, P', T', and R' can be simplified, leading to the dynamic programming problem

$$f(N,P,T,R) = \max_{E_1,E_2,E_3,E,P',T',S',R'}\left\{\frac{1}{1-\beta\theta}\log\left[\left(1-\frac{E_2}{A_2N}-\frac{E_3}{A_3N}\right)^{1-\theta-\nu}E^{\nu}\right] + \beta\big[f\big(N',P',T',R'\big)+\alpha\log\big(1-\Delta S'\big)\big]\right\},$$

s.t.

$$E = \left(\kappa_1 E_1^{\rho} + \kappa_2 E_2^{\rho} + \kappa_{,3} E_3^{\rho}\right)^{1/\rho},$$
$$N' = (1+g)N,$$
$$R' = R - E_1 \geq 0,$$
$$P' = P + \phi_L(E_1 + E_2),$$
$$T' = (1-\phi)T + (1-\phi_L)\phi_0(E_1 + E_2),$$
$$S' = P' + T'.$$

The value function $f(N, P, T, R)$ is represented by a four-dimensional Chebyshev polynomial and solved numerically using value function iteration. The above simplification significantly reduces the computational burden from solving a dynamic max-min game, allowing us to utilize the parallel toolbox of MATLAB on an eight-processor computer. Value function iteration stops when $\|f^{k+1} - f^k\|_\infty < 1 \times 10^{-6}$; by the contraction mapping property, the numerical error $\|f - f^k\|_\infty \leq \frac{1}{1-\beta}\|f^{k+1} - f^k\|_\infty < \frac{1\times 10^{-6}}{1-0.985^{10}} \approx 7.1 \times 10^{-6}$.[29] Table 2 reports the grid specifications (rectangular domain of P, T, R, and N) used in the complete model for the normal distribution case.[30]

TABLE 2. Grid specifications of Chebyshev polynomial approximation (normal distribution of γ).

	($R_0^{\text{oil}} = 253.8$ GtC) and Unlimited Coal; $\alpha = 0.01, \infty$	Unlimited Oil and Unlimited Coal; $\alpha = 0.01, \infty$	($R_0^{\text{oil}} = 253.8$ GtC) and $R_0^{\text{coal}} = 666$ GtC); $\alpha = 0.01, \infty$
No. of grid points for P	6	6	6
No. of grid points for T	7	7	7
No. of grid points for R^{oil}	15	NA	10
No. of grid points for R^{coal}	NA	NA	10
No. of grid points for N	10	10	10
$[P_1, P_{\text{end}}]$	[0, 1000]	[0, 3000]	[0, 1000]
$[T_1, T_{\text{end}}]$	[0, 1000]	[0, 3000]	[0, 1000]
$[R_1^{\text{oil}}, R_{\text{end}}^{\text{oil}}]$	[0.5, 255]	NA	[0, 330]
$[R_1^{\text{coal}}, R_{\text{end}}^{\text{coal}}]$	NA	NA	[0, 770]
$[N_1, N_{\text{end}}]$	[0.8, 100]	[0.8, 100]	[0.8, 100]

[29]Note that we only report the numerical error due to the stopping of contraction iteration, and not the numerical error due to Chebyshev interpolation. For some of the difficulties associated with measuring numerical errors of higher order interpolations, such as Chebyshev interpolation; see Santos and Vigo-Aguiar (1998).

[30]Our numerical algorithm imposes the natural constraints that $N \geq 0$ and $R \geq 0$. Since the resource constraint for oil/gas is binding given the initial stock, $R = 253$ GtC, and since the curvature of the value function with respect to (w.r.t.) R increases as R approaches zero, we increased the number of nodes for R from 15 to 30, but obtained identical results. The numerical procedure allows T and P to be negative. We also used negative 100 as the lowest grid point for both P and T and found no noticeable change in the numerical results.

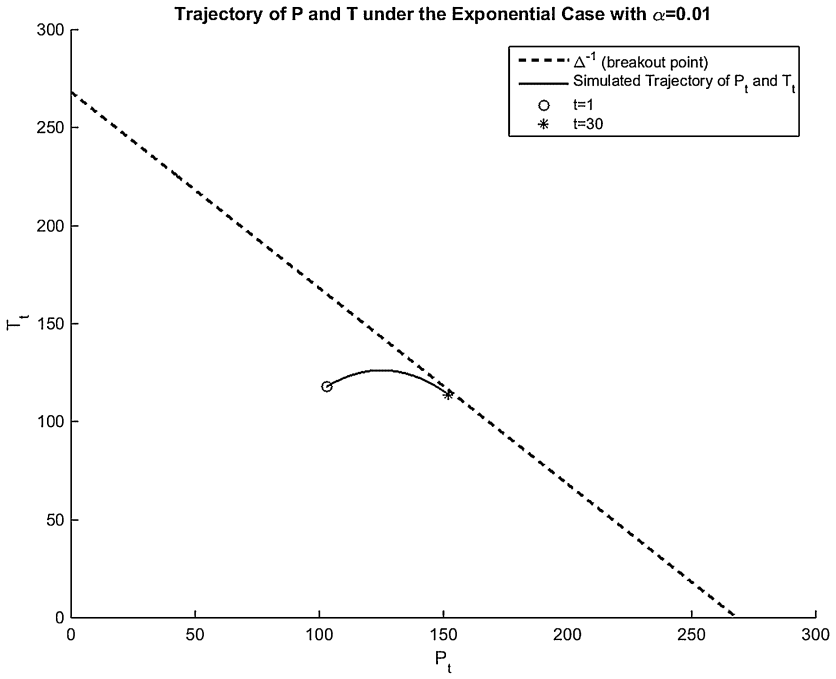

FIGURE 9. Trajectory of P and T with exponential distribution and $\alpha = 0.01$.

A.2.2 *Exponential distribution of* γ We used the standard Chebyshev method to approximate the value function under a normal distribution assumption regarding γ. This approximation estimates the value function when P and T lie in a rectangular area. However, this method cannot be applied when the approximating distribution for γ is exponential, as the domain of P and T is triangular in that case. In the exponential case, the value function goes to $-\infty$ as $P + T$ approaches the breakout point, $1/\Delta$. Therefore, the domain of P and T is contained in $\{(P, T)|P + T \leq 1/\Delta\}$. In particular, the breakout point under $\alpha = 0.01$ is $1/\Delta = 268$ GtC, which is very close to the maximum of the trajectory of $P_t + T_t$ in the simulation horizon, as is illustrated in Figure 9. As a result, we are not able to find a rectangular area for P and T that (i) is large enough to contain the trajectory of interest for $\{P_t, T_t\}$ and (ii) does not intersect with the breakout point, $1/\Delta$.

We address this issue by transforming the state space for P and T into the state space of X and Y by rotating the coordinates 45° counterclockwise, as depicted in Figure 9. This rotation reshapes the triangular domain for P and T into a rectangular domain for X and Y, thereby allowing us to apply the standard rectangular Chebyshev approximation. Specifically, let $\theta^{\text{rot}} = 45°$ and define

$$X = \cos\big(\theta^{\text{rot}}\big)P + \sin\big(\theta^{\text{rot}}\big)T,$$
$$Y = -\sin\big(\theta^{\text{rot}}\big)P + \cos\big(\theta^{\text{rot}}\big)T.$$

TABLE 3. Grid specifications of Chebyshev polynomial approximation (exponential distribution of γ).

	($R_0 = 253.8$ GtC); $\alpha = 0.01$	($R_0 = 253.8$ GtC); $\alpha = 0.1, 1, 100, \infty$
No. of grid points for X	6	6
No. of grid points for Y	7	7
No. of grid points for R	15	15
No. of grid points for N	10	10
$[X_1, X_{\text{end}}]$	[0, 189.13]	[0, 700]
$[Y_1, Y_{\text{end}}]$	[−189.63, 189.63]	[−700, 700]
$[R_1, R_{\text{end}}]$	[0.5, 255]	[0.5, 255]
$[N_1, N_{\text{end}}]$	[0.8, 100]	[0.8, 100]

This transformation implies

$$P = \cos\bigl(\theta^{\text{rot}}\bigr)X - \sin\bigl(\theta^{\text{rot}}\bigr)Y,$$
$$T = \sin\bigl(\theta^{\text{rot}}\bigr)X + \cos\bigl(\theta^{\text{rot}}\bigr)Y.$$

In addition, let $\tilde{f}(N, X, Y, R) = f(N, P(X, Y), T(X, Y), R)$. Then the computational problem can be transformed as

$$\tilde{f}(N, X, Y, R) = \max_{E_1, E_2, E_3, E, X', Y', S', R'} \left\{ \frac{1}{1-\beta\theta} \log\left[\left(1 - \frac{E_2}{A_2 N} - \frac{E_3}{A_3 N} \right)^{1-\theta-\nu} E^{\nu} \right] + \beta\bigl[\tilde{f}\bigl(N', X', Y', R'\bigr) + \alpha \log\bigl(1 - \Delta S'\bigr)\bigr] \right\},$$

s.t.

$$E = \bigl(\kappa_1 E_1^{\rho} + \kappa_2 E_2^{\rho} + \kappa_3 E_3^{\rho}\bigr)^{1/\rho},$$
$$N' = (1+g)N,$$
$$R' = R - E_1 \geq 0,$$
$$X' = \frac{\sqrt{2}}{2}\bigl[\phi_L + (1-\phi_L)\phi_0\bigr](E_1 + E_2) + \frac{1}{2}(X - Y) + \frac{1-\phi}{2}(X + Y),$$
$$Y' = \frac{\sqrt{2}}{2}\bigl[-\phi_L + (1-\phi_L)\phi_0\bigr](E_1 + E_2) - \frac{1}{2}(X - Y) + \frac{1-\phi}{2}(X + Y),$$
$$S' = \sqrt{2}X'.$$

Furthermore, to calculate the marginal externalities from P and T, we need to express $\frac{\partial f}{\partial P}$ and $\frac{\partial f}{\partial T}$ in terms of $\frac{\partial \tilde{f}}{\partial X}$ and $\frac{\partial \tilde{f}}{\partial Y}$:

$$\frac{\partial f}{\partial P} = \frac{\partial \tilde{f}}{\partial X}\frac{\partial X}{\partial P} + \frac{\partial \tilde{f}}{\partial Y}\frac{\partial Y}{\partial P} = \frac{\sqrt{2}}{2}\left(\frac{\partial \tilde{f}}{\partial X} - \frac{\partial \tilde{f}}{\partial Y} \right),$$
$$\frac{\partial f}{\partial T} = \frac{\partial \tilde{f}}{\partial X}\frac{\partial X}{\partial T} + \frac{\partial \tilde{f}}{\partial Y}\frac{\partial Y}{\partial T} = \frac{\sqrt{2}}{2}\left(\frac{\partial \tilde{f}}{\partial X} + \frac{\partial \tilde{f}}{\partial Y} \right).$$

Similar to the case of normal distribution of γ, the value function iteration method is employed to solve for f numerically with a similar stopping threshold and thus a similar numerical error. Table 3 reports the grid specifications (rectangular domain of X, Y, R, and N) used in the complete model for the exponential distribution case.

References

Acemoglu, D., P. Aghion, L. Bursztyn, and D. Hemous (2012), "The environment and directed technical change." *American Economic Review*, 102 (1), 131–166. [824]

Adao, B., B. Narajabad, and T. Temzelides (2012), "A model with spillovers in the adaptation of new renewable technologies." Working paper, James A. Baker III Institute for Public Policy. [849]

Anderson, E., W. Brock, L. P. Hansen, and A. Sanstad (2014), "Robust analytical and computational explorations of coupled economic-climate models with carbon-climate response." Working Paper 13-05, RDCEP. [824]

Bommier, A. (2006), "Uncertain lifetime and intertemporal choice: Risk aversion as a rationale for time discounting." *International Economic Review*, 47 (4), 1223–1246. [824]

Bommier, A., B. Lanz, and S. Zuber (2015), "Models-as-usual for unusual risks? On the value of catastrophic climate change." *Journal of Environmental Economics and Management*, 74, 1–22. [824]

Bommier, A. and J.-C. Rochet (2006), "Risk aversion and planning horizons." *Journal of the European Economic Association*, 4 (4), 708–734. [824]

Boswell, R. and T. S. Collett (2011), "Current perspectives on gas hydrate resources." *Energy & Environmental Science*, 4, 1206–1215. [823]

Funke, M. and M. Paetz (2010), "Environmental policy under model uncertainty: A robust optimal control approach." *Climatic Change*, 107 (3–4), 225–239. [824]

Gerlagh, R. and M. Liski (2014), "Carbon prices for the next hundred years." Manuscript, Tilburg University. [824]

Golosov, M., J. Hassler, P. Krusell, and A. Tsyvinski (2014), "Optimal taxes on fossil fuel in general equilibrium." *Econometrica*, 82 (1), 41–88. [822]

Hansen, L. P. and T. J. Sargent (2008), *Robustness*. Princeton University Press, Princeton, NJ. [821, 850]

Hansen, L. P. and T. J. Sargent (2010), "Wanting robustness in macroeconomics." In *Handbook of Monetary Economics*, Vol. 3, Chapter 20, 1097–1157, North-Holland, Amsterdam. [824]

Hartley, P., K. Medlock III, T. Temzelides, and X. Zhang (2016), "Energy sector innovation and growth." *The Energy Journal*, 37 (1). [823, 849]

IPCC (2014), *Climate Change 2014: Synthesis Report. Contribution of Working Groups I, II and III to the Fifth Assessment Report of the Intergovernmental Panel on Climate Change*. IPCC, Geneva, Switzerland. [840]

Jacobson, D. (1973), "Optimal stochastic linear systems with exponential performance criteria and their relation to deterministic differential games." *IEEE Transactions on Automatic Control*, AC-18 (2), 124–131. [824]

Nordhaus, W. and J. Boyer (2000), *Warming the World: Economic Models of Climate Change*. MIT Press, Cambridge, MA. [824]

Rezai, A. and F. van der Ploeg (2014), "Intergenerational inequality aversion, growth and the role of damages: Occam's rule for the global tax." OxCarre Research Paper 150, Oxford University. [822]

Santos, M. S. and J. Vigo-Aguiar (1998), "Analysis of a numerical dynamic programming algorithm applied to economic models." *Econometrica*, 66 (2), 409–426. [853]

Stern, N. (2007), *The Economics of Climate Change: The Stern Review*. Cambridge University Press, Cambridge. [824]

Stern, N. (2013), "The structure of economic modeling of the potential impacts of climate change: Grafting gross underestimation of risk onto already narrow science models." *Journal of Economic Literature*, 51 (3), 838–859. [841]

van den Bijgaart, I., R. Gerlagh, and M. Liski (2013), "A simple formula for the social cost of carbon." Working Paper Series 836, Fondazione Eni Enrico Mattei. [822]

van der Ploeg, F. (1993), "A closed-form solution for a model of precautionary saving." *Review of Economic Studies*, 60 (2), 385–395. [824]

Whittle, P. (1981), "Risk-sensitive linear/quadratic/Gaussian control." *Advances in Applied Probability*, 13 (4), 764–777. [824]

Whittle, P. (2002), "Risk-sensitivity, a strangely pervasive concept." *Macroeconomic Dynamics*, 6 (1), 5–18. [824]

Co-editor Karl Schmedders handled this manuscript.

Submitted June, 2014. Final version accepted December, 2015.